NASA MEMO 10-11-58L

NASA

MEMORANDUM

AERODYNAMIC CHARACTERISTICS IN SIDESLIP OF A LARGE-SCALE 49° SWEPTBACK WING-BODY-TAIL CONFIGURATION WITH BLOWING APPLIED OVER THE FLAPS AND WING LEADING EDGE

By H. Clyde McLemore

Langley Research Center
Langley Field, Va.

NATIONAL AERONAUTICS AND SPACE ADMINISTRATION
WASHINGTON
October 1958
Declassified April 12, 1961

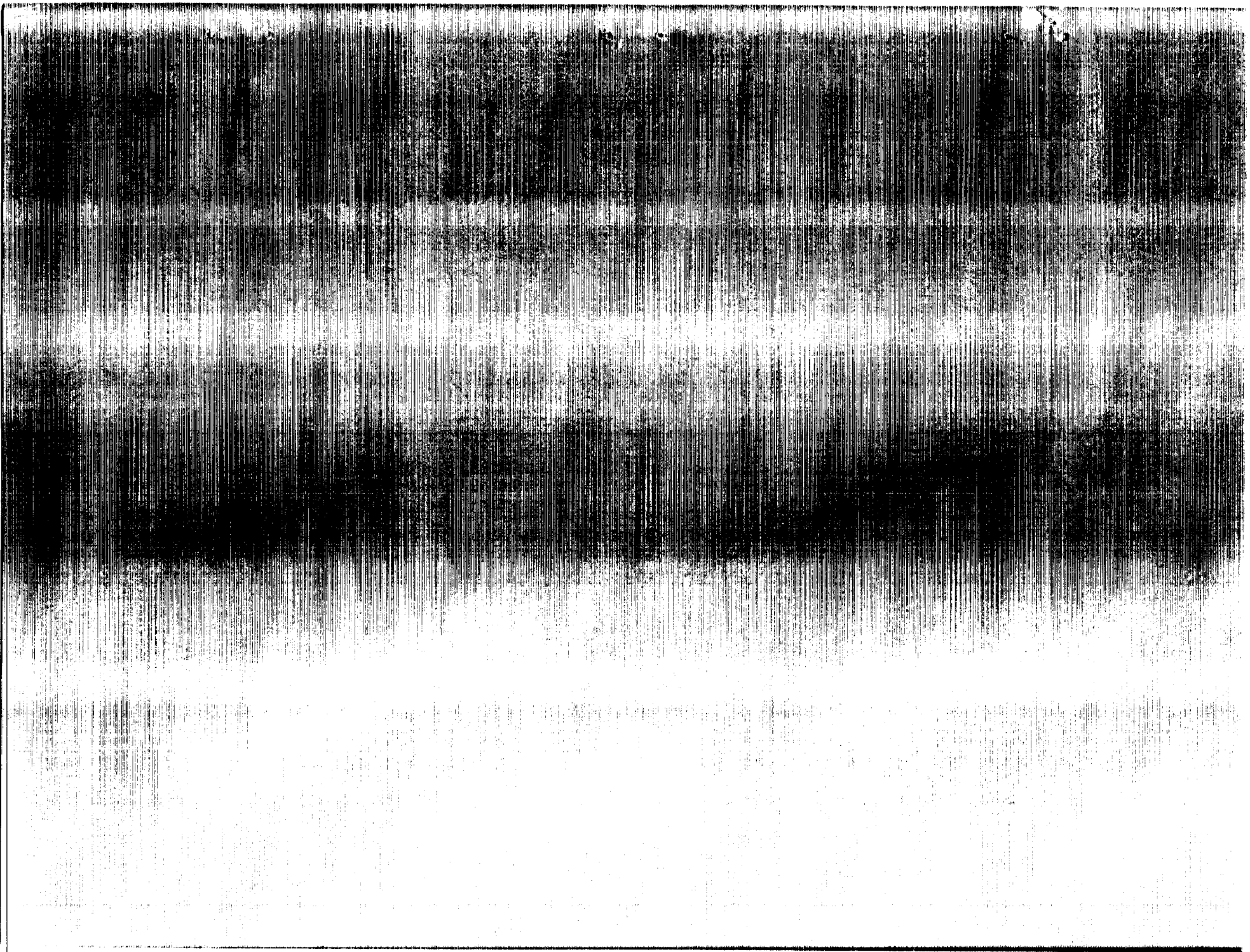

NATIONAL AERONAUTICS AND SPACE ADMINISTRATION

NASA MEMO 10-11-58L

AERODYNAMIC CHARACTERISTICS IN SIDESLIP OF A LARGE-SCALE 49° SWEPTBACK WING-BODY-TAIL CONFIGURATION WITH BLOWING APPLIED OVER THE FLAPS AND WING LEADING EDGE*

By H. Clyde McLemore

SUMMARY

An investigation has been conducted in the Langley full-scale tunnel to determine the aerodynamic characteristics in sideslip of a large-scale 49° sweptback wing-body-tail configuration having wing leading-edge and flap-blowing boundary-layer control. The wing and tails had an aspect ratio of 3.5, a taper ratio of 0.3, and NACA 65A006 airfoil sections parallel to the plane of symmetry. The tests were conducted over a range of angles of attack of about -5° to 28° for sideslip angles of 0°, -5.06°, -10.15°, and -15.18°. Lateral and longitudinal stability and control characteristics were obtained for a minimized blowing rate. The Reynolds number of the tests was 5.2×10^6, corresponding to a Mach number of 0.08.

The results of the investigation showed that sideslip to angles of about -15° did not require, from a consideration of the longitudinal characteristics, blowing rates over the wing leading edge or flap greater than that established as minimum at zero sideslip. The optimum configuration was laterally and directionally stable through the complete lift-coefficient range including the stall; however, maximum lift for sideslip angles greater than about 5° was seriously limited by a deficiency of lateral control. Blowing over the leading edge of the retreating wing in sideslip at a rate greater than that established as minimum at zero sideslip was ineffective in improving the lateral control characteristics. The optimum configuration at zero sideslip had no hysteresis of the aerodynamic parameters upon recovery from stall.

*Title, Unclassified.

INTRODUCTION

The successful application of blowing boundary-layer control at the flap and leading edge of swept-wing fighter-airplane configurations for improved low-speed performance has been demonstrated in a number of wind-tunnel and flight investigations. (See refs. 1 to 7.) The studies to date, however, have concentrated primarily on the achievement of greater usable maximum lift and improved longitudinal stability and control. It is not an uncommon experience, however, for highly swept wing configurations to have lateral and directional deficiencies in sideslip at low speeds, and for this reason it was considered necessary to evaluate the overall low-speed characteristics of such a configuration in sideslip. Of particular interest to the designer of the boundary-layer control system is the question as to whether the minimum energy bleed requirements established at zero sideslip would be adequate for sideslip in the approach and landing and whether a differential wing leading-edge blowing arrangement could be considered for lateral control in sideslip.

As a result of the studies reported in references 1 and 2, it was considered necessary to conduct a few additional tests at zero sideslip of combinations of wing leading-edge droop and blowing rates to insure an absolute minimum energy blowing system as a basis for evaluating the effects of sideslip on such a boundary-layer control system.

An investigation has been conducted, therefore, in the Langley full-scale tunnel to determine the aerodynamic characteristics in sideslip of a large-scale research model incorporating minimum blowing over the wing leading edge and over trailing-edge flaps.

The model used in the investigation (basically the same as that used in refs. 2 and 3) was a large-scale, thin, 49° sweptback wing-body-tail configuration. The wing and tails had an aspect ratio of 3.5, a taper ratio of 0.3, and NACA 65A006 airfoil sections parallel to the plane of symmetry.

Tests of the investigation were made for the angle-of-attack range of approximately -5° to 28° for a sideslip-angle range of 0° to -15.18°. The Reynolds number of the tests was 5.2×10^6 which corresponds to a Mach number of 0.08.

SYMBOLS

All data are referred to the stability system of axes with the moment center about the projection of the 25-percent mean-aerodynamic-chord point on the longitudinal axis of the body.

b	wing span, ft
c	local wing chord measured parallel to plane of symmetry, ft
$\bar{c}$	mean aerodynamic chord of wing, ft
$\bar{c}_t$	mean aerodynamic chord of horizontal tail, ft
i_t	angle of incidence of horizontal tail (trailing edge up, negative), deg
q	free-stream dynamic pressure, $\frac{1}{2}\rho_\infty V_\infty^2$, lb/sq ft
Q	volume flow of air ejected from blowing slot, cu ft/sec
S	area of wing, sq ft
V_j	velocity of ejected air at blowing slot, ft/sec
V_∞	free-stream velocity, ft/sec
z	perpendicular distance of horizontal tail from extended wing-chord plane (above wing-chord plane, positive), ft
α	angle of attack, deg
β	angle of sideslip, deg
δ_a	aileron deflection (measured perpendicular to hinge line; down deflections considered positive for left- or right-hand aileron), deg
δ_f	flap deflection (measured perpendicular to hinge line), deg
δ_n	wing leading-edge droop deflection (measured perpendicular to hinge line), deg
ρ_j	mass density of air ejected from slot, slugs/cu ft
ρ_∞	mass density of free-stream air, slugs/cu ft
C_D	drag coefficient (drag equivalent of pumping power not included), Drag/qS
C_L	lift coefficient, Lift/qS

$C_{L,max}$ maximum lift coefficient

C_Y side-force coefficient, $\frac{\text{Side force}}{qS}$

C_l rolling-moment coefficient, $\frac{\text{Rolling moment}}{qSb}$

C_m pitching-moment coefficient about $\bar{c}/4$, $\frac{\text{Pitching moment}}{qS\bar{c}}$

C_n yawing-moment coefficient, $\frac{\text{Yawing moment}}{qSb}$

C_μ blowing-momentum coefficient, $\frac{Q\rho_j V_j}{qS}$

$C_{l_\beta} = \frac{\partial C_l}{\partial \beta}$

$C_{n_\beta} = \frac{\partial C_n}{\partial \beta}$

$C_{Y_\beta} = \frac{\partial C_Y}{\partial \beta}$

I inboard portion of wing leading-edge droop (0.142b/2 to 0.466b/2)

C center portion of wing leading-edge droop (0.466b/2 to 0.669b/2)

O outboard portion of wing leading-edge droop (0.669b/2 to 1.000b/2)

Subscripts:

f flap

K knee

L left hand

R right hand

MODEL

A large-scale research model having the geometric characteristics shown in figure 1 was used in the investigation. The wing and tail (both horizontal and vertical) had a leading-edge sweep of 49°, an aspect ratio of 3.5, a taper ratio of 0.3, and NACA 65A006 airfoil sections parallel to the plane of symmetry. The horizontal tail was mounted 8.4 inches ($z/\bar{c} = -0.077$) below the wing-chord plane extended at a tail length of $1.43\bar{c}$. A photograph of the model mounted for tests in the Langley full-scale tunnel is given as figure 2.

The wing leading-edge flow-control device used was a 0.17c, full-span droop (flap) with a blowing slot located in the knee of the droop (fig. 3(a)). The droop was divided into three spanwise sections (fig. 1) - inboard, center, and outboard (referred to as sections I, C, and O, respectively, in this report) - for the purpose of regulating the spanwise extent and amount of blowing and providing for a variable-deflection wing leading-edge droop.

The wing was also equipped with 0.24c ailerons and semispan flaps with a blowing slot located in the wing just forward of the flap (fig. 3(b)). The aileron geometry was the same as that of the flap (fig. 3(b)) but because of the very large values of pitching moment that resulted from blowing over the ailerons (ref. 1), the blowing slot at the aileron was not used.

The high-pressure blowing boundary-layer-control air-supply system and flow measurement procedures used in the investigation were the same as that used and fully described in reference 2.

TESTS

The force data, taken on the tunnel six-component scale-balance system, were measured over the angle-of-attack range from approximately -5° to 28° for angles of sideslip of 0°, -5.06°, -10.15°, and -15.18°. Reynolds number of the tests was 5.2×10^6 which corresponds to a Mach number of 0.08.

Tests were conducted at zero sideslip to refine further the wing leading-edge flow-control system used in reference 2. The refinement consisted of systematically deflecting sections of the nose droop and varying the rate of knee blowing from the compartments formed by droop sections I, C, and O. Minimum blowing rates were determined for both the wing leading edge and the flap. The optimum configuration

was then tested through the sideslip range 0° to -15.18°. For each sideslip angle the ailerons and horizontal tail were deflected through the range -15° to 40° and 0° to -40°, respectively, to determine the static lateral and longitudinal stability and control characteristics.

A few tests were conducted with various rates and combinations of spanwise extent of wing leading-edge blowing over the left-hand wing for sideslip angles of 0°, -5.06°, and -15.18° to determine the value of this type of blowing control as a lateral-control device.

CORRECTIONS

The data have been corrected for airstream misalinement, buoyancy, and jet boundary effects. In order to make the present data equivalent to a self-contained system, the drag was corrected by adding the term ρQV which is the drag equivalent of taking on board the mass of air (ρQ) which had an original velocity, with relation to the model, of V. This correction was necessary because the air ejected through the blowing slots was admitted to the model from a source outside of the airstream.

DISCUSSION

Longitudinal Characteristics

Previous wind-tunnel tests of the research model with the horizontal tail on the wing-chord plane extended (ref. 2) have shown the high-lift configurations to have a "pitch-up" at maximum lift. Preliminary downwash surveys indicated a more favorable downwash field for a horizontal tail below the wing-chord plane; therefore, in an attempt to alleviate the aforementioned pitch-up, further tests were conducted on the subject model with the horizontal tail lowered an arbitrary 8.4 inches ($z/\bar{c} = -0.077$) below the wing-chord plane extended. As shown in figure 4 (the only data directly comparable with previous chord-plane extended tail data), lowering the horizontal tail did not improve the pitch-up of the high-lift configuration at $C_{L,max}$; this result indicates that the tail was not lowered enough. Because the lowered tail appeared to improve the stability prior to $C_{L,max}$, the lowered tail position was used throughout the remainder of the tests.

In order to review briefly the general effects of blowing boundary-layer control on the longitudinal characteristics of the subject model (more detailed results given in refs. 1, 2, and 3), the lift, drag, and pitching-moment characteristics with and without flap and knee blowing

are shown in figure 5. Also shown in figure 5 is the effect of shutting off the inboard blowing at the knee of the drooped-wing leading edge in another attempt to control the pitch-up at $C_{L,max}$ by creating a favorable chordwise center-of-pressure shift on the inboard portion of the wing. Shutting off the inboard knee blowing air, however, did not particularly improve the stability characteristics but caused a reduction in $C_{L,max}$ of the order of 0.07. It is concluded from figure 5, therefore, that for a blowing system utilizing both knee and flap blowing, "full-span" knee blowing, at some minimum rate at least, will be required to maintain the best possible high-lift characteristics.

In order to illustrate the gross effect that knee blowing has on the air flow over the model, visual and photographic flow studies were made for the high-lift configuration with no knee blowing on the right-hand wing. The results of these flow studies at zero sideslip and zero aileron deflection for several angles of attack are shown in figure 6. The angles of attack and values of lift coefficient given for the left- and right-hand wing (fig. 6) are those that would have resulted if both wings had either knee and flap blowing or only flap blowing. It can be readily seen that knee blowing has the very powerful effect of preventing air-flow separation over the wing leading-edge and outboard sections of a highly swept wing to high angles of attack. At a moderate angle of attack ($\alpha = 11.2^{\circ}$), although the total lift is not particularly affected by not having knee blowing, the flow over outboard located ailerons without knee blowing would result in poor lateral control characteristics.

A study of the force and pressure distribution data and movies of the flow patterns on the wing of references 2 and 3 indicated that the combination of wing leading-edge droop angle and knee blowing rate could be further refined and thereby improve the model high-lift characteristics. For the present tests, therefore, the various sections of nose droop and rates of knee blowing were systematically varied to establish a near-optimum configuration for the remainder of the tests. The tests showed that neither the minimum blowing rates of the knee blowing air nor the flap blowing rate could be reduced more than that established as minimum in reference 2 without incurring a considerable loss in $C_{L,max}$. The wing leading-edge droop angles of reference 2, however, were found not to be optimum. Shown in figure 7 are the results of the leading-edge droop-angle variation tests for the previously determined minimum flap and knee blowing rates. From the curves of figure 7, the wing leading-edge droop configuration was selected for the remainder of the tests. The configuration selected (hereinafter referred to as the optimum configuration) produced the highest untrimmed maximum lift coefficient of those tested $\left(C_{L,max} = 1.63\right)$ and is described as follows:

δ_n, deg, for -			δ_f, deg	$C_{\mu,f}$	$C_{\mu,K}$ for -		
					I	C	O
I	C	O	60	0.012	0.001	0.002	0.009
40	50	56					

It should be noted that the unstable stall was nearly eliminated for the optimum configuration. A slightly greater outboard droop deflection angle might have resulted in a stable stall.

Shown also in figure 7 is the effect of reducing angle of attack from values beyond the stall to values well below the stall. With knee blowing it can be seen that there is no hysteresis whatsoever and thus knee blowing would be very desirable from the pilot's viewpoint. In the event of stall, the airplane would completely recover its unstalled characteristics as soon as the angle of attack is reduced below the angle of stall.

For the high-lift configuration just discussed, longitudinal characteristics were determined for the lowered tail position for a range of horizontal-tail deflection angles from 0° to -40°. As determined from preliminary data, the $0.25\bar{c}$ moment center location gave a static margin of the order of $0.20\bar{c}$ to $0.25\bar{c}$ which resulted in pitching-moment-coefficient values, near $C_{L,max}$, that were too large to be trimmed by a normal tail. This static margin is considerably larger than that used for conventional fighter-type airplanes; therefore the pitching-moment data of figure 8 are computed about a center-of-gravity position of $0.37\bar{c}$ (static margin at low values of C_L of approximately $0.07\bar{c}$). For this center-of-gravity position the model, with the aforementioned minimized blowing rates, could be longitudinally trimmed to a $C_{L,max}$ of about 1.4. This, however, would not leave the pilot any margin of lift before pitch-up and would, therefore, limit trimmed $C_{L,max}$ to some value lower than 1.4. The static margin required for the pilot to trim to a C_L of about 1.4 and still have a margin of trimmed C_L before stall would be the order of $0.03\bar{c}$ to $0.05\bar{c}$.

For the optimum configuration, established at zero sideslip, tests in sideslip (-5.06°, -10.15°, and -15.18°) were conducted through the complete angle-of-attack range (approximately -5° through the stall). Visual flow studies and force measurements, although not presented, were made with both increasing and decreasing rates of flap and knee blowing on the left and right wings in order to determine the blowing rates required to control wing leading edge or flap air flow separation. From these flow studies and force measurements it was determined that the

minimum blowing rates were about the same as those required at zero sideslip. Increasing the left- or right-hand knee blowing rate did not improve the flow or force characteristics, whereas decreasing the knee blowing rate was detrimental. Increasing or decreasing the blowing rate over the flap in sideslip also showed that the minimum blowing rate was about the same as that required at zero sideslip.

The results of the tests in sideslip of the optimum configuration are shown in figure 9. For angles of sideslip greater than about 5° the lift-curve slope is seen to decrease with increasing sideslip angle while the drag at high lift coefficients is increased. Maximum lift is also reduced for sideslip angles greater than about 5°. It is interesting to note that sideslip improved the longitudinal stability characteristics of the model and for the largest angle of sideslip tested (-15.18°) the configuration had very good longitudinal stability characteristics through the complete lift-coefficient range, including the stall.

The results of tests to determine the horizontal-tail effectiveness in sideslip are shown in figure 10 for the original center-of-gravity position of $0.25\bar{c}$. Sideslip near $C_{L,max}$ caused only a slight reduction in the tail effectiveness and this, coupled with the improved longitudinal stability at the stall, would allow the pilot to require less margin of lift before $C_{L,max}$; therefore, the maximum trimmed lift coefficient in sideslip would still be about 1.4. This statement will have to be qualified, as shown later, in that the lateral characteristics in sideslip may limit the maximum trimmed lift coefficient to some value lower than 1.4.

Lateral and Directional Characteristics

The variation of the basic lateral and directional characteristics of the model with and without boundary-layer control with angle of sideslip are presented in figure 11. The data without any blowing and that with flap blowing only are presented for two main purposes: first, they represent the condition in which a pilot might find himself should he lose boundary-layer control in a high-lift attitude; and second, although the configuration (droop- and flap-deflection angles) is not one which would be selected without boundary-layer control, these data are nevertheless presented for their quantitative value.

It should be noted that the lateral and directional coefficients (C_l, C_n, and C_Y) are not always zero at zero angle of sideslip for the knee and flap blowing and the flap blowing only configurations. These values (other than zero) are probably the result of slight blowing

asymmetries between the left- and the right-hand wings. The data analyses in this report which utilize these coefficients consider the zero sideslip values.

A summary of the static lateral and directional stability characteristics with and without boundary-layer control is given in figure 12. The data of figure 12 were obtained by taking slopes of the basic data (fig. 11) through sideslip angles of 0° to -2°. In general, for the knee- and flap-blowing and no-blowing configurations the model is laterally and directionally stable through the complete lift-coefficient range including the stall. For the no-blowing configuration, separation of flow occurs at the wing leading edge and/or knee and results in a rapid loss of effective dihedral for C_L values greater than 1.1. The configuration becomes laterally unstable at a C_L value of 1.2. The directional characteristics are about the same as those discussed for the lateral stability characteristics except that the no-blowing configuration does not become directionally unstable through the complete lift-coefficient range, including the stall.

The effect of the loss of boundary-layer control on the lateral and directional stability characteristics is not directly shown in figure 12. A knee and flap blowing configuration, however, would probably be operating in an angle-of-attack and C_L range well above the angle of attack for $C_{L,max}$ of the flap-blowing-only and the no-boundary-layer control configurations, and a loss in boundary-layer control could cause the airplane to become uncontrollable.

Lateral Control

The use of blowing boundary-layer control over inboard flaps or outboard over the wing leading edge has been shown in references 1 and 3 to be a powerful means of increasing the effectiveness of outboard trailing-edge ailerons at high angles of attack. A more thorough study of the effect of blowing at the knee of an outboard wing leading-edge flap on the aileron characteristics over a range of sideslip angles has been conducted in this current investigation.

The basic data of this investigation, with and without boundary-layer control, are presented in figures 13 to 16 for several aileron (both left- and right-hand) deflection and sideslip angles. The flap-blowing-only and the no-boundary-layer control data are presented to illustrate the general improvement knee blowing makes on the lateral control characteristics.

For analysis purposes the zero aileron deflection data with knee and flap blowing are repeated, for the sideslip angles investigated, in

figure 17. Included on the curves of figure 17 are the maximum lift points and, using combined maximum increments of rolling-moment coefficient of the left- and right-hand ailerons (generally -15° and 40° deflection, respectively) at a given angle of attack, the points of maximum lift with trimmed rolling moments are also noted. The zero sideslip curve is considered the reference data and at zero sideslip the roll can be trimmed through $C_{L,max}$. As shown in figure 17, the maximum angle of attack (and therefore $C_{L,max}$) is seriously limited in the higher sideslip conditions by insufficient lateral control.

In an attempt to increase the angle of attack for lateral trim, several tests were conducted with various sections of the knee blowing air of the left-hand (advancing) wing shut off. It was believed that, by proper programing of this air shutoff, larger increments of rolling moment could be obtained than from the ailerons. The results of these tests for sideslip angles of 0°, -5.06°, and -15.18° are shown in figure 18. From these data it can be readily seen that knee blowing has only a minor effect on the rolling-moment characteristics in the low angle-of-attack range, that is, where there is little or no wing leading-edge flow separation problem. At high angles of attack, however, progressive reduction of the knee blowing air supply is seen to produce large increments of C_l. From the data of figure 18 it can be seen that sufficiently large rolling moments are produced at the high angles of attack to counteract the roll produced by sideslip by shutting off the advancing wing knee blowing air. (For instance, above an angle of attack of about 20° at -15.18° sideslip, a sufficient increment of C_l is available for trim.) For this type of lateral control system, however, there exists, in the moderate angle-of-attack range (about 12° to 20° for a sideslip angle of -15.18°), a region in which sufficient rolling moment for lateral trim would not be produced by shutting off the advancing wing knee blowing air. As a single roll control device, therefore, this knee blowing air shutoff method would not be acceptable.

A few tests were conducted with the right-hand (retreating) wing knee blowing air rate increased in an attempt to alleviate the loss in lift of the retreating wing and thereby reduce the large rolling moments. Although these data are not presented, the retreating wing knee blowing rate was doubled and even tripled at high angles of attack, but the rolling-moment-coefficient values and $C_{L,max}$ remained essentially unchanged. It is concluded, therefore, that blowing over the knee of the retreating wing at a rate greater than that established as minimum at zero sideslip is also not a satisfactory method for improving the lateral control characteristics of a highly swept wing in sideslip.

CONCLUSIONS

Results of tests in the Langley full-scale tunnel to determine the aerodynamic characteristics in sideslip of a large scale, 49° sweptback wing-body-tail configuration having wing leading edge and flap blowing boundary-layer control indicate the following conclusions:

1. Sideslip to angles of about -15° did not require, from a consideration of the longitudinal characteristics, blowing rates over the wing leading edge or flap greater than that established as minimum at zero sideslip.

2. The optimum configuration was laterally and directionally stable through the complete lift-coefficient range, including the stall.

3. Maximum lift of the optimum configuration in sideslip was seriously limited by a deficiency of lateral control for sideslip angles greater than about 5°.

4. Blowing over the leading edge of the retreating wing in sideslip at a rate greater than that established as minimum at zero sideslip was ineffective in improving the lateral control characteristics.

5. Loss of boundary-layer control at high values of lift coefficient and sideslip could result in an uncontrollable airplane.

6. The optimum configuration at zero sideslip had no hysteresis of the aerodynamic parameters upon recovery from stall.

Langley Research Center,
National Aeronautics and Space Administration,
Langley Field, Va., July 29, 1958.

REFERENCES

1. McLemore, H. Clyde, and Fink, Marvin P.: Blowing Over the Flaps and Wing Leading Edge of a Thin 49° Swept Wing-Body-Tail Configuration in Combination With Leading-Edge Devices. NACA RM L56E16, 1956.

2. Fink, Marvin P., and McLemore, H. Clyde: High-Pressure Blowing Over Flap and Wing Leading Edge of a Thin Large-Scale 49° Swept Wing-Body-Tail Configuration in Combination With a Drooped Nose and a Nose With a Radius Increase. NACA RM L57D23, 1957.

3. McLemore, H. Clyde, and Fink, Marvin P.: Surface Pressure Distributions on a Large-Scale 49° Sweptback Wing-Body-Tail Configuration With Blowing Applied Over the Flaps and Wing Leading Edge. NACA RM L57K25, 1958.

4. Anderson, Seth B., Quigley, Hervey C., and Innis, Robert C.: Flight Measurements of the Low-Speed Characteristics of a 35° Swept-Wing Airplane With Blowing-Type Boundary-Layer Control on the Trailing-Edge Flaps. NACA RM A56G30, 1956.

5. Quigley, Hervey C., Hom, Francis W. K., and Innis, Robert C.: A Flight Investigation of Area-Suction and Blowing Boundary-Layer Control on the Trailing-Edge Flaps of a 35° Swept-Wing Carrier-Type Airplane. NACA RM A57B14, 1957.

6. James, Harry A., and Maki, Ralph L.: Wind-Tunnel Tests of the Static Longitudinal Characteristics at Low Speed of a Swept-Wing Airplane With Blowing Flaps and Leading-Edge Slats. NACA RM A57D11, 1957.

7. Hickey, David H., and Aoyagi, Kiyoshi: Large-Scale Wind-Tunnel Tests of an Airplane Model With a 45° Sweptback Wing of Aspect Ratio 2.8 Employing High-Velocity Blowing Over the Leading- and Trailing-Edge Flaps. NACA RM A58A09, 1958.

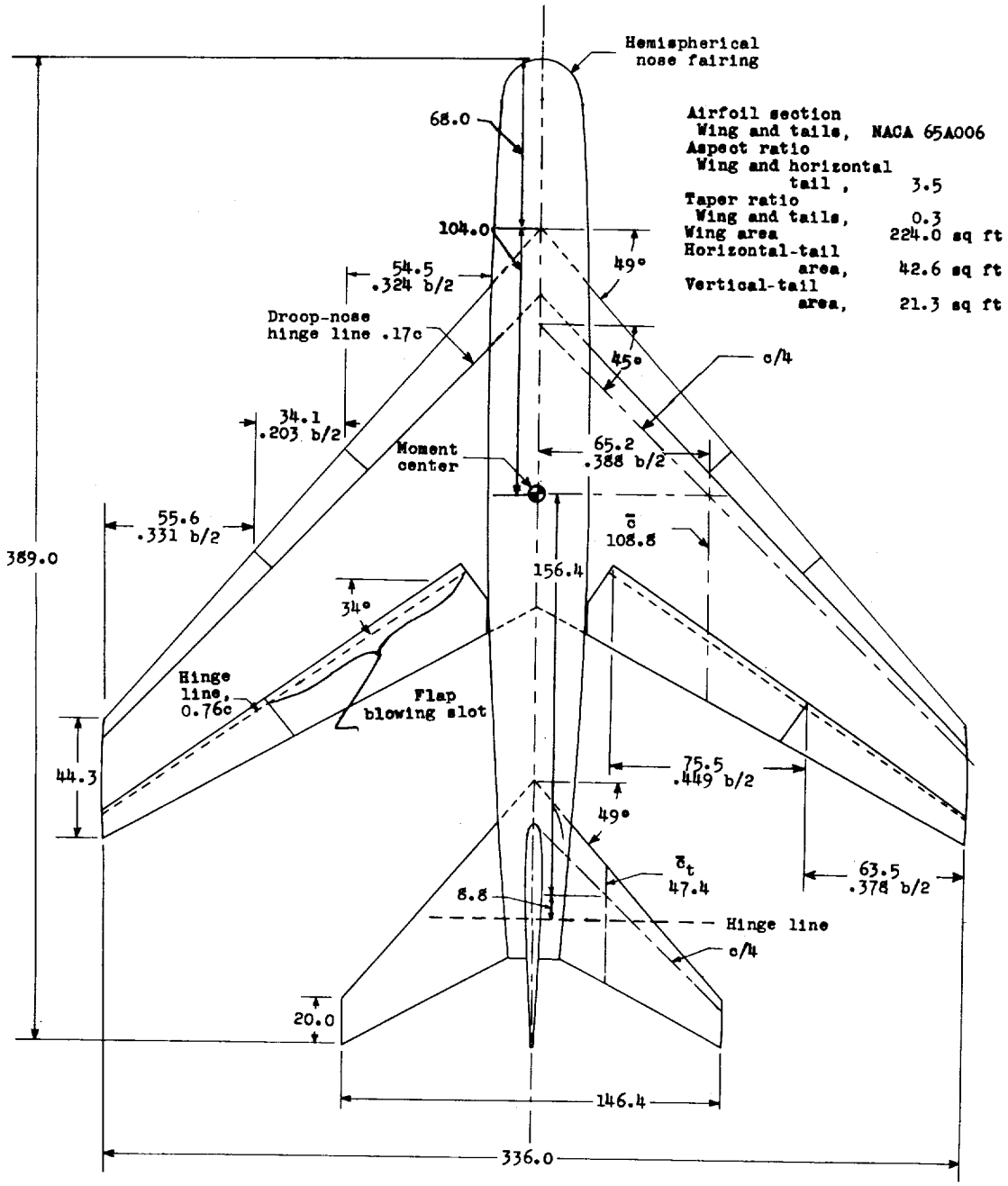

Figure 1.- Geometric characteristics of the model. All dimensions are in inches unless otherwise indicated.

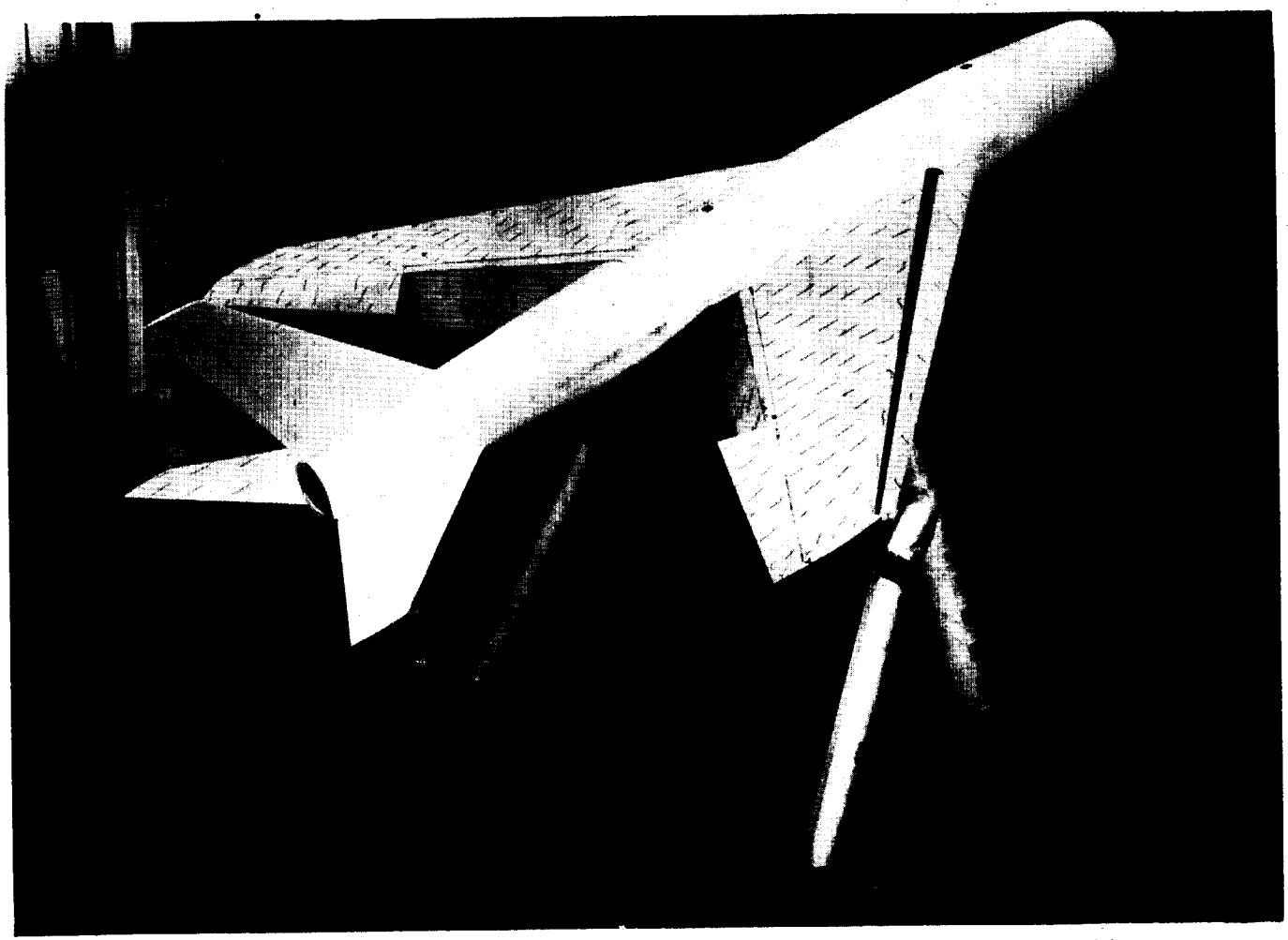

L-57-4093

Figure 2.- General view of model mounted for tests in the Langley full-scale tunnel with flow-survey tufts attached.

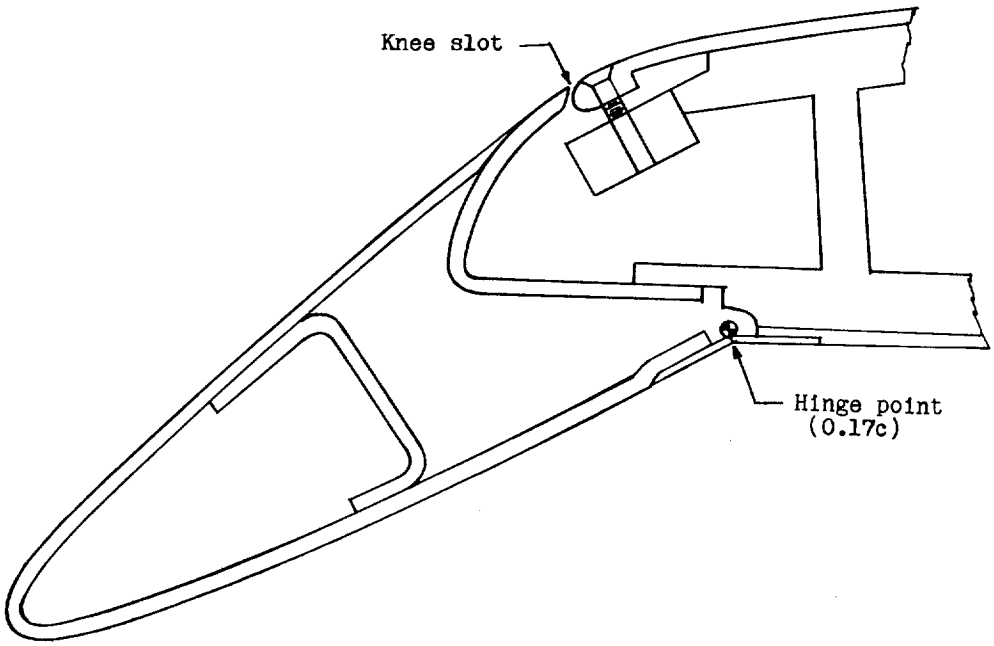

(a) Typical droop-nose section.

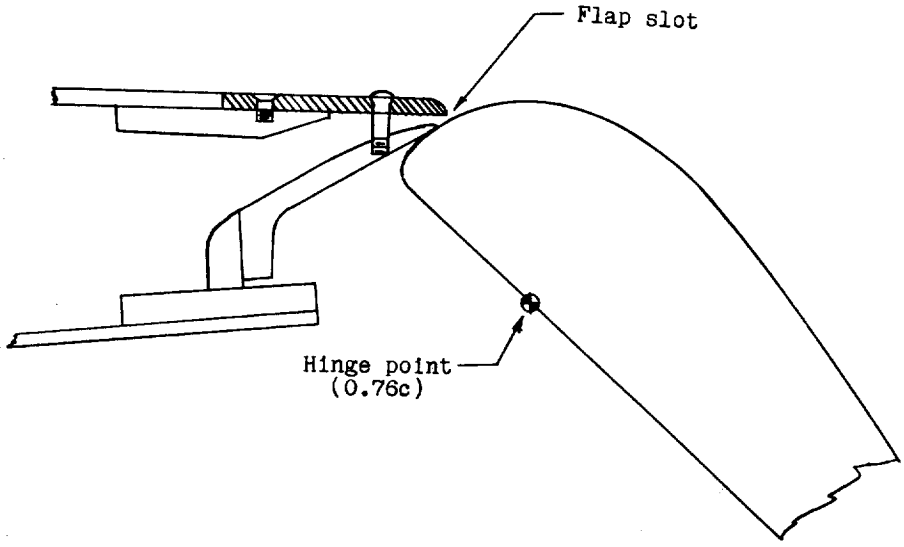

(b) Typical flap-slot section.

Figure 3.- Sectional views of the high-lift and flow-control devices.

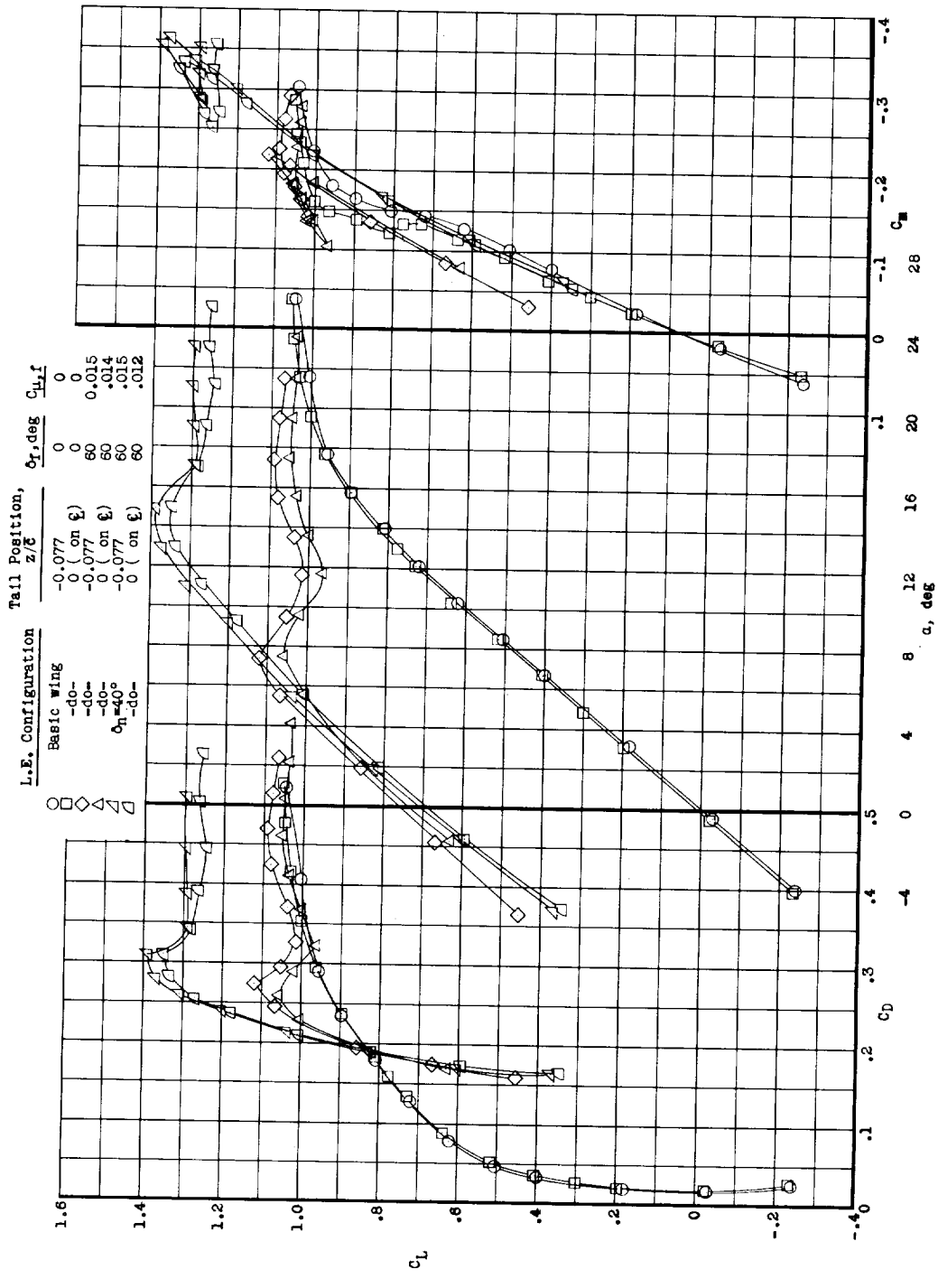

Figure 4.- Effect of lowering the horizontal tail on the longitudinal aerodynamic characteristics of several configurations. $\beta = 0^o$; $\delta_a = 0^o$; $i_t = 0^o$.

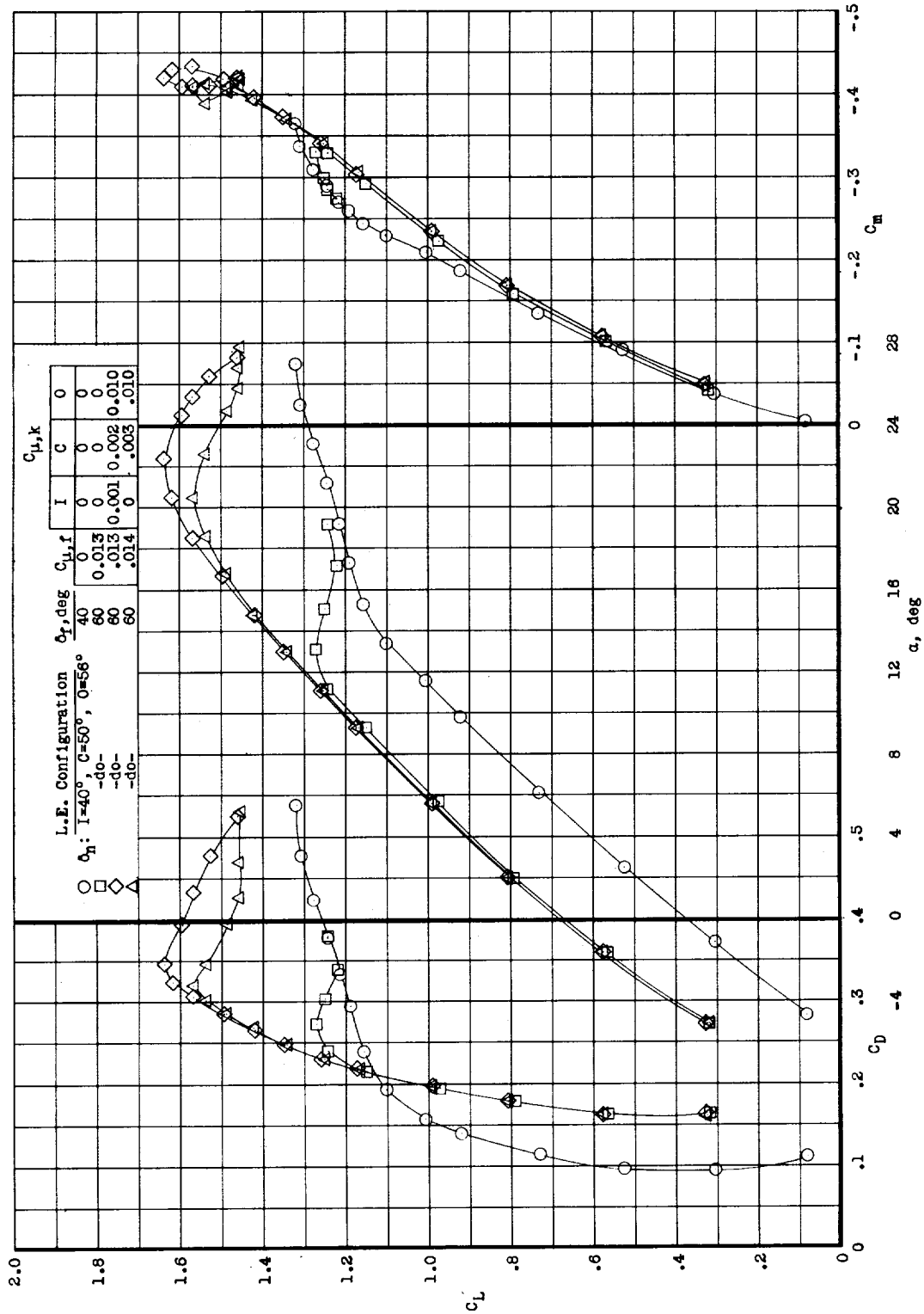

Figure 5.- Effect of flap and knee blowing on the longitudinal aerodynamic characteristics of the drooped-wing leading-edge configuration. $\beta = 0^o$; $\delta_a = 0^o$; $i_t = 0^o$.

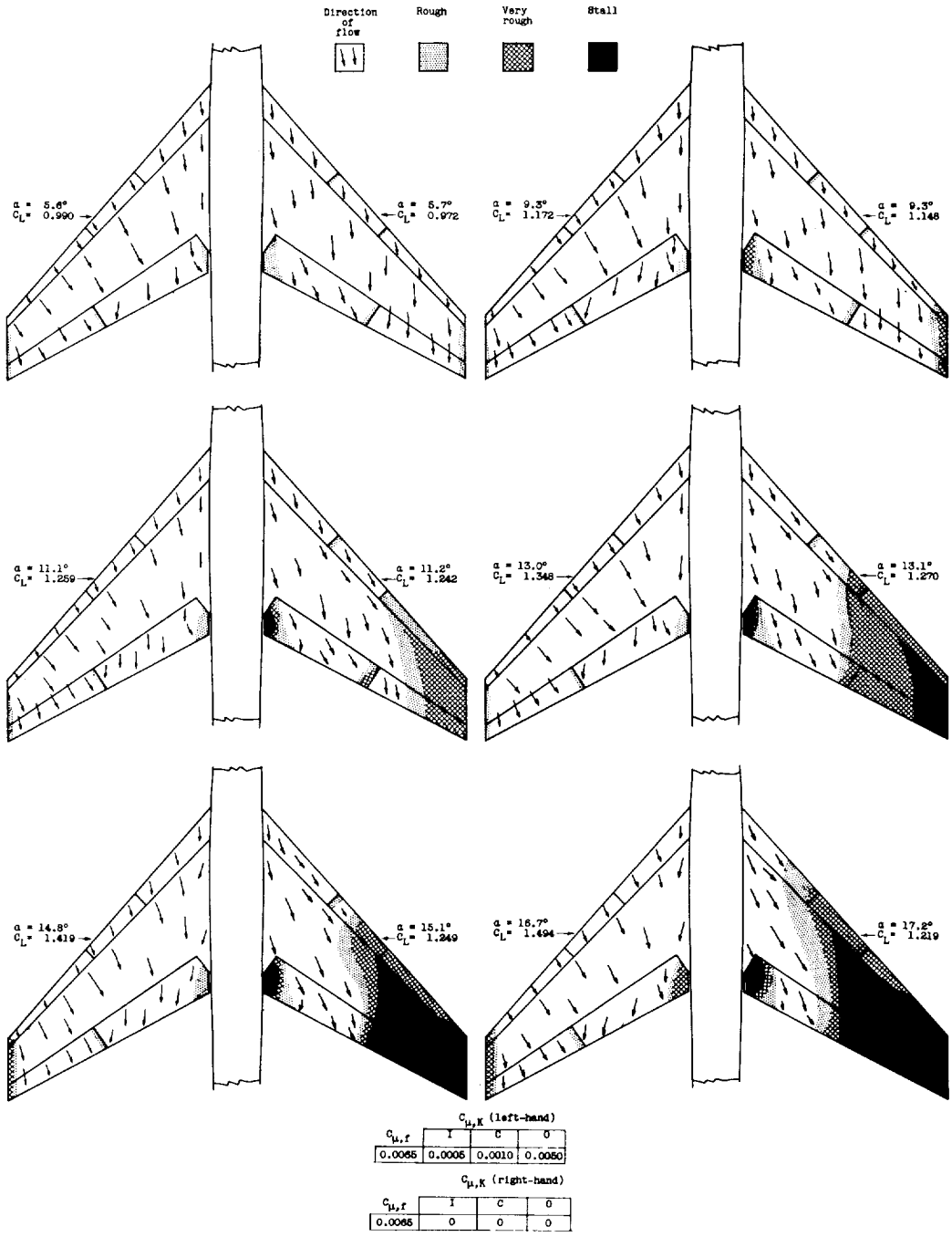

Figure 6.- Flow visualization studies of the model with knee and flap blowing on the left-hand wing and with flap blowing only on the right-hand wing. δ_n: I = 40°, C = 50°, and O = 56°; δ_a = 0°; i_t = 0°; δ_f = 60°.

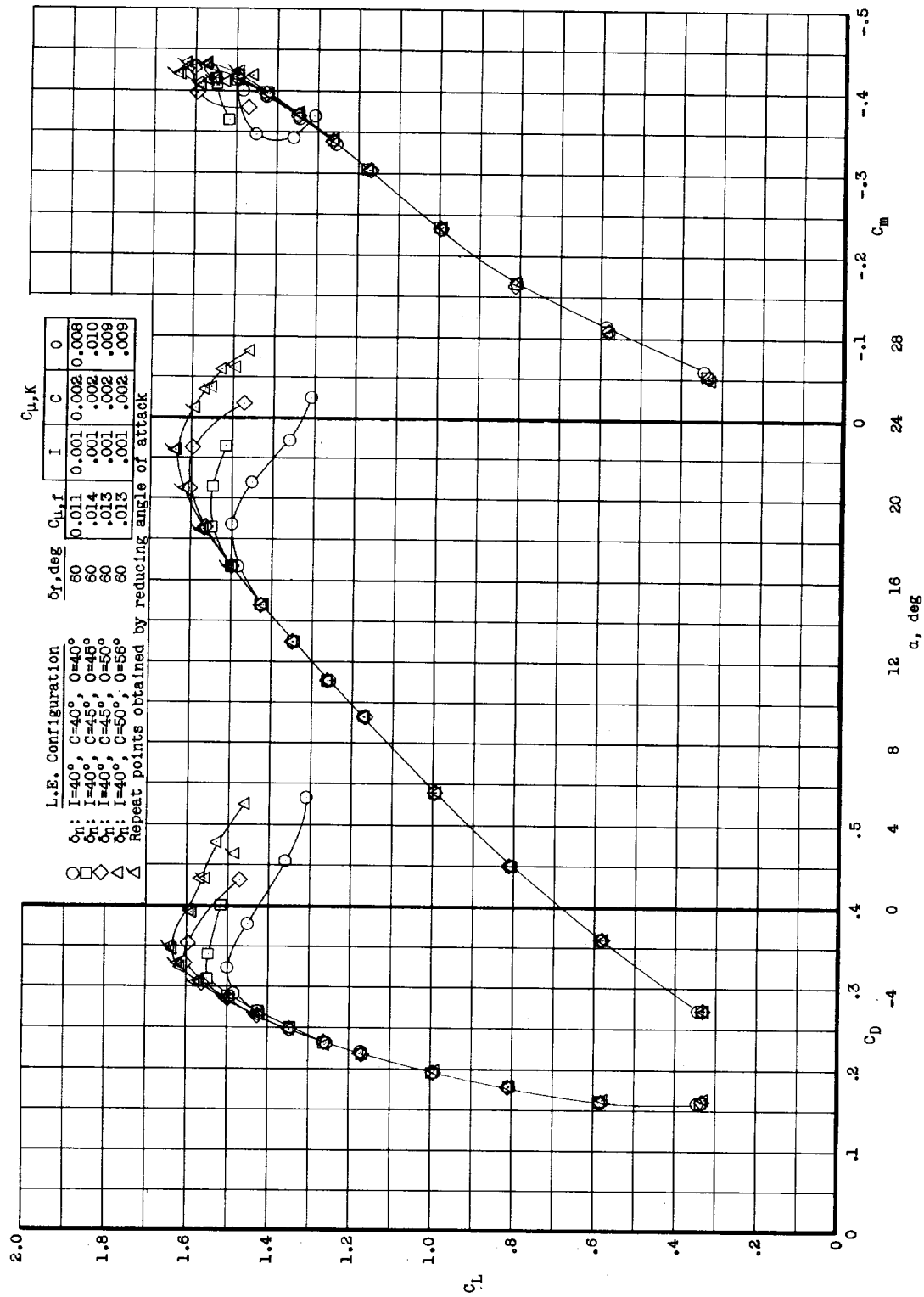

Figure 7.- Effect of varying the wing leading-edge droop angle on the longitudinal aerodynamic characteristics. $\beta = 0^{\circ}$; $\delta_a = 0^{\circ}$; $i_t = 0^{\circ}$.

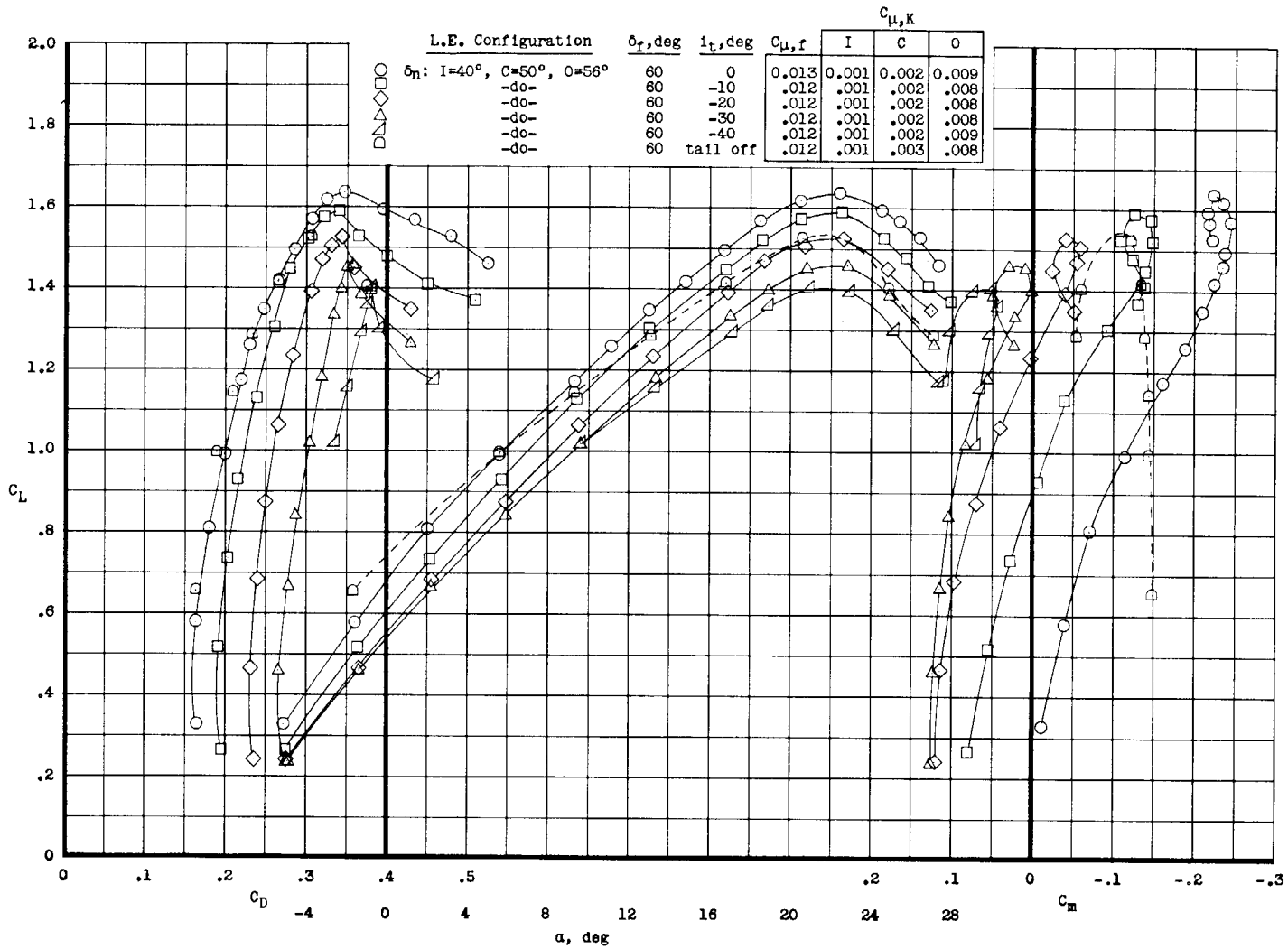

Figure 8.- Variation of the longitudinal aerodynamic characteristics with horizontal-tail deflection for a center-of-gravity position of 0.37$\bar{c}$. Knee and flap blowing; $\delta_a = 0^o$.

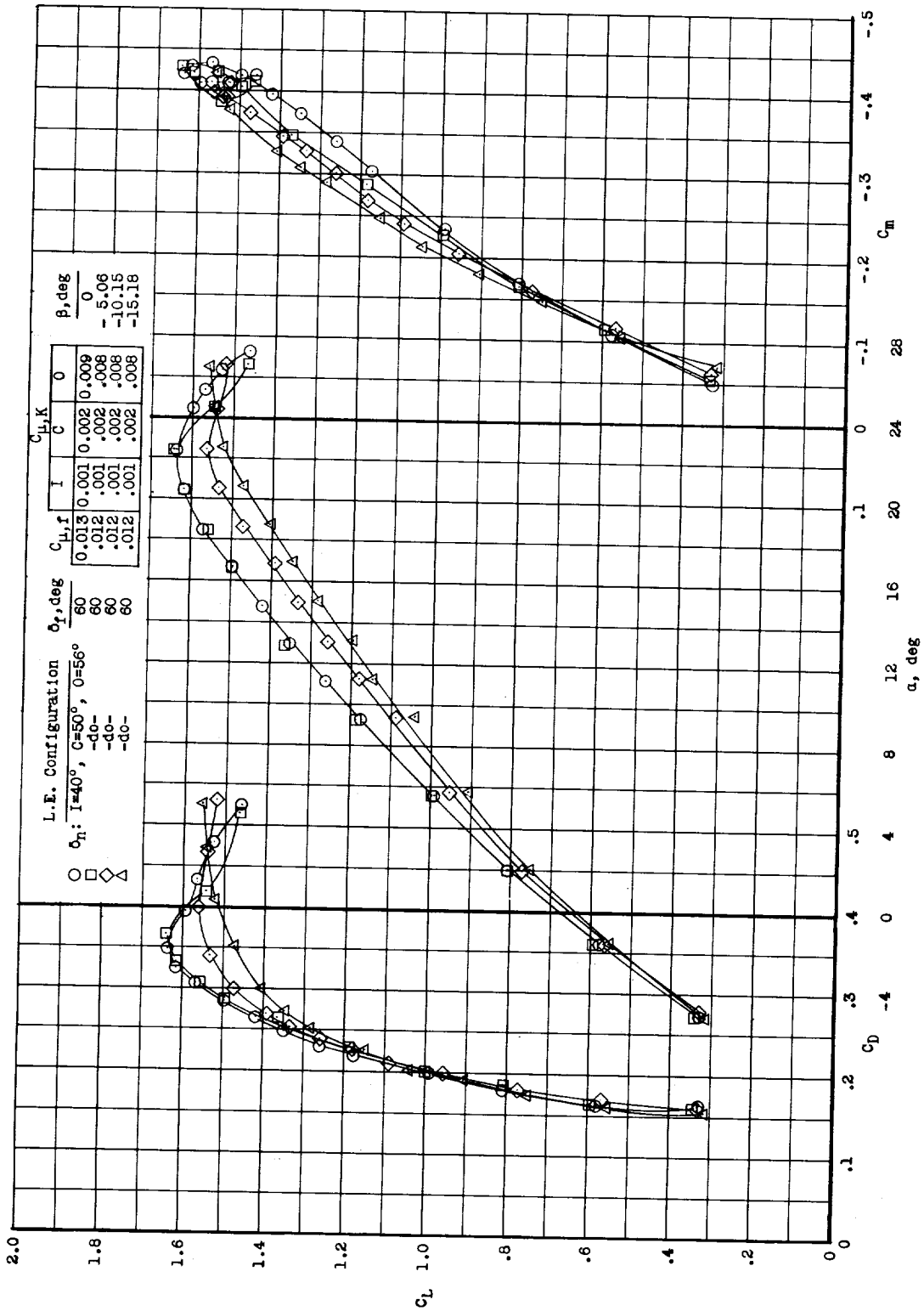

Figure 9.- Variation of the static longitudinal aerodynamic characteristics with angle of sideslip. Knee and flap blowing; $\delta_a = 0^o$; $i_t = 0^o$.

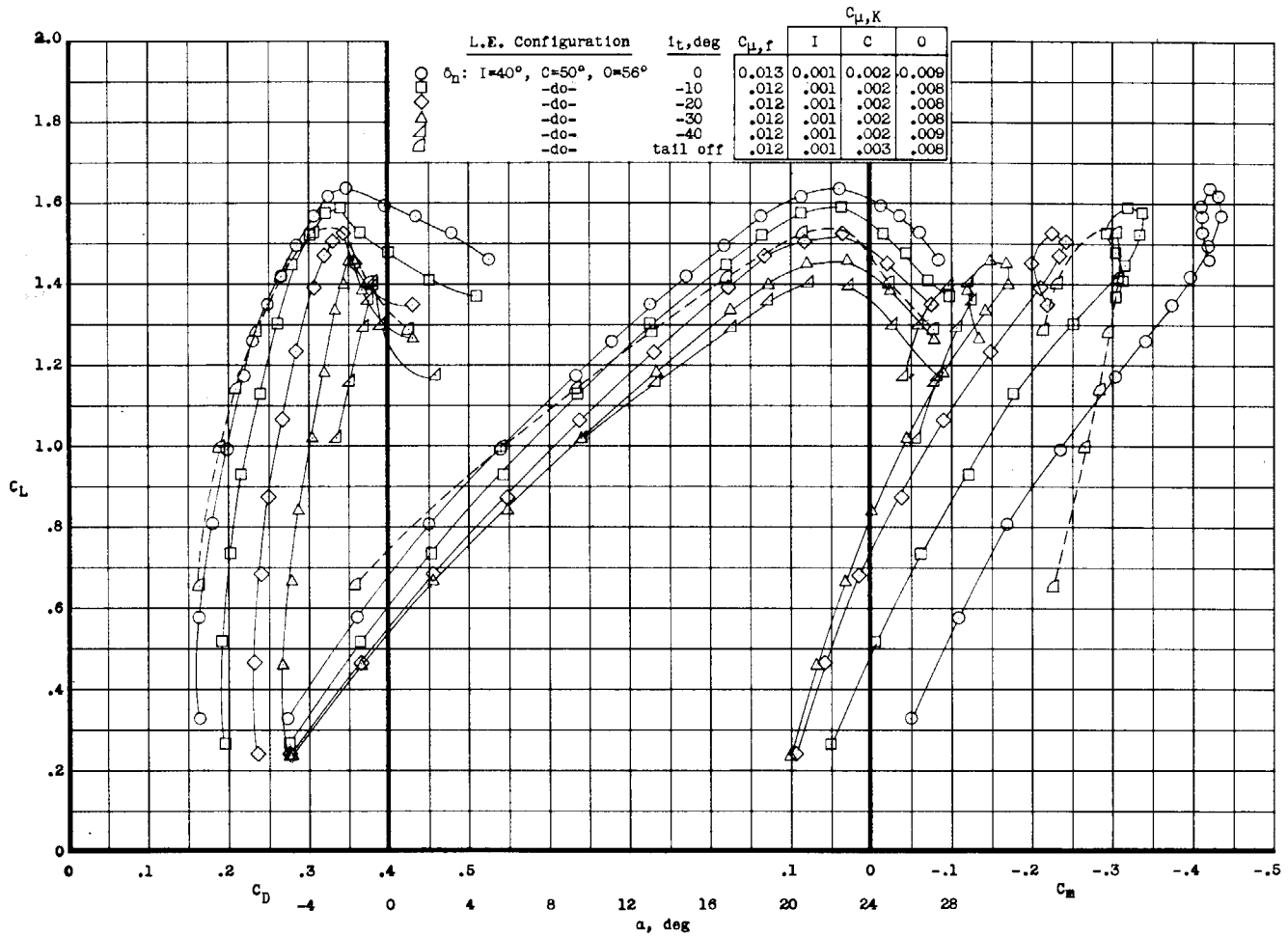

(a) $\beta = 0^\circ$.

Figure 10.- Effect on the longitudinal aerodynamic characteristics of deflecting the horizontal tail for several sideslip angles. Knee and flap blowing; $\delta_a = 0^\circ$; $\delta_f = 60^\circ$.

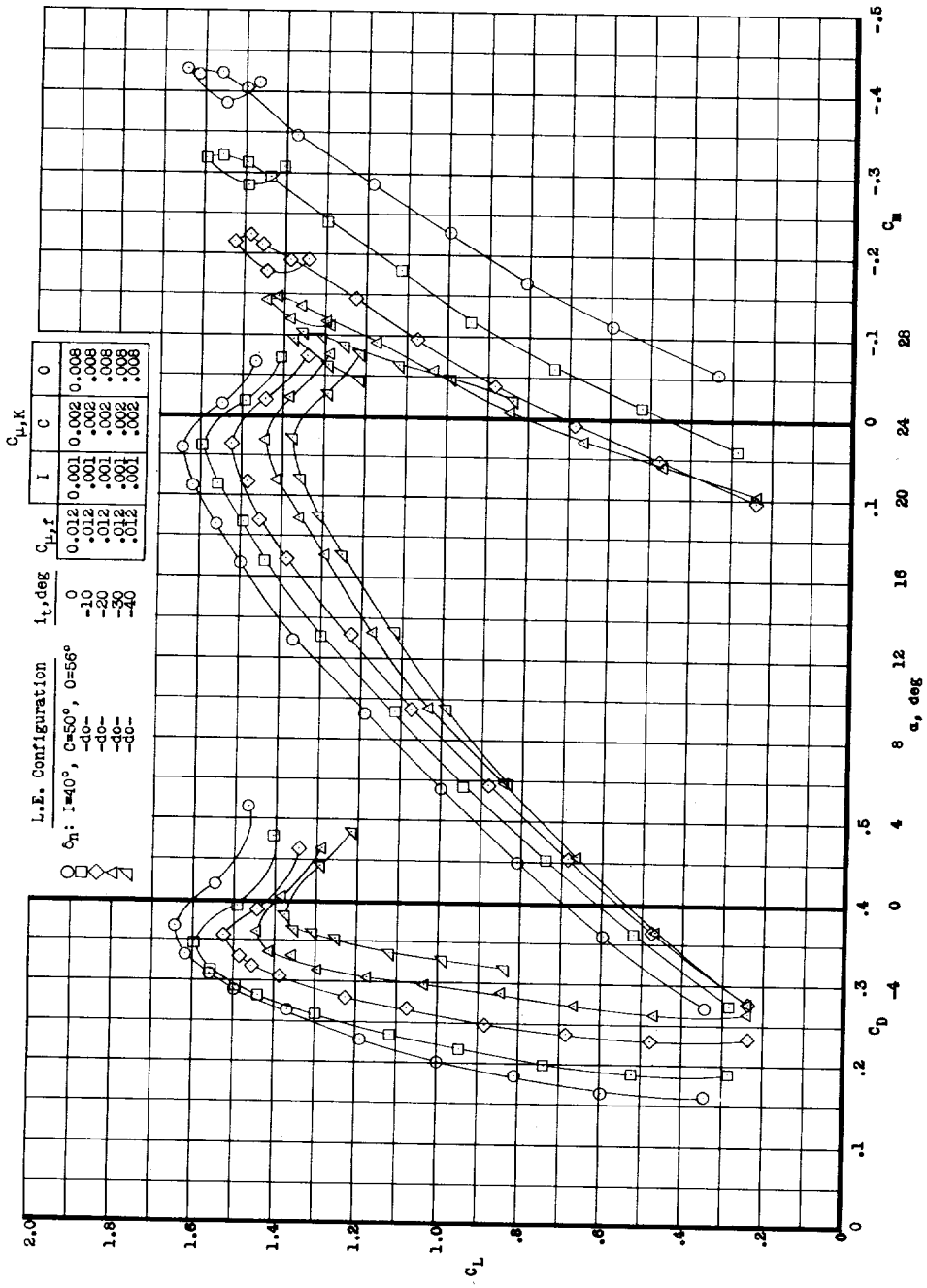

(b) $\beta = -5.06°$.

Figure 10.- Continued.

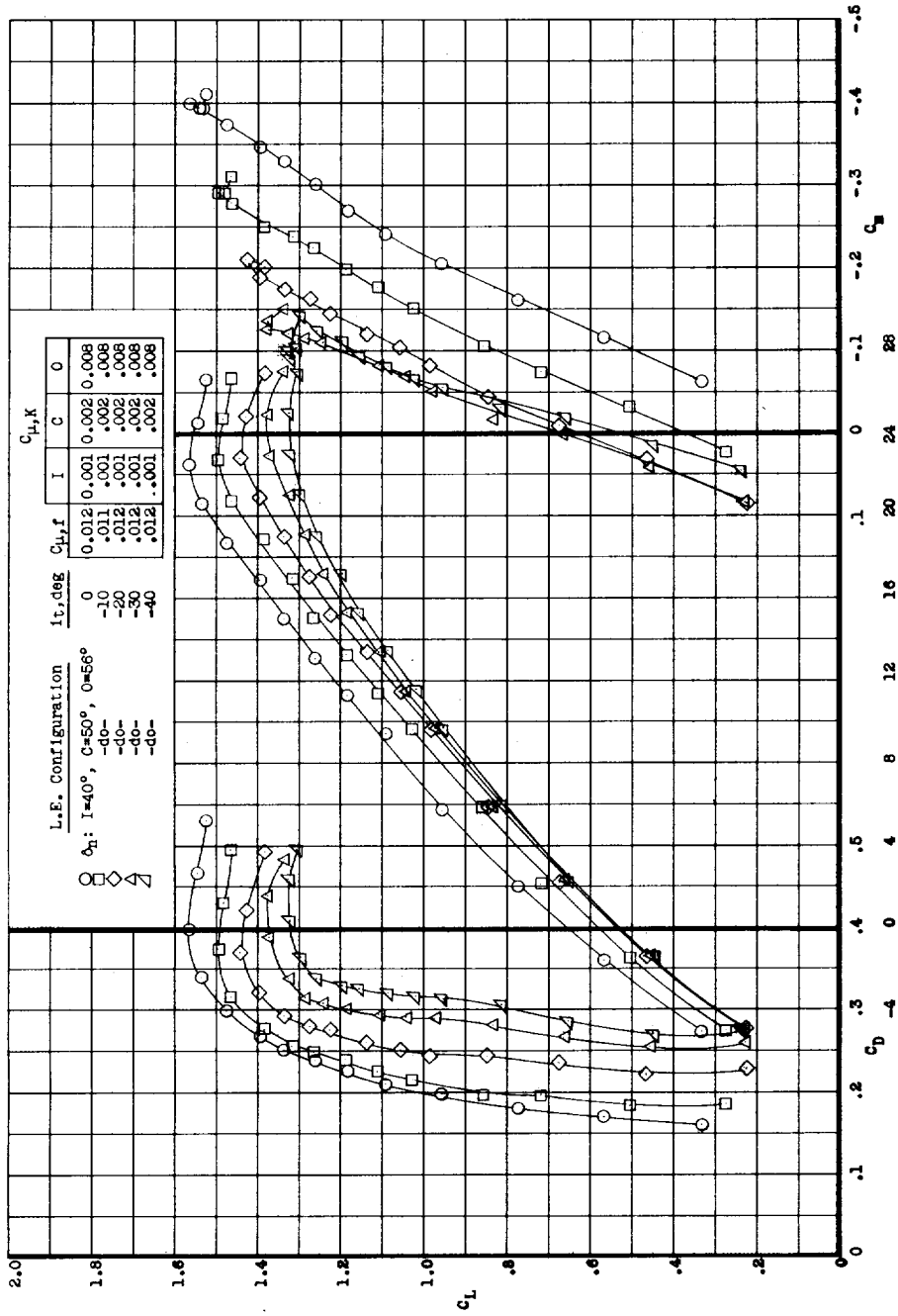

(c) $\beta = -10.15°$.

Figure 10.- Continued.

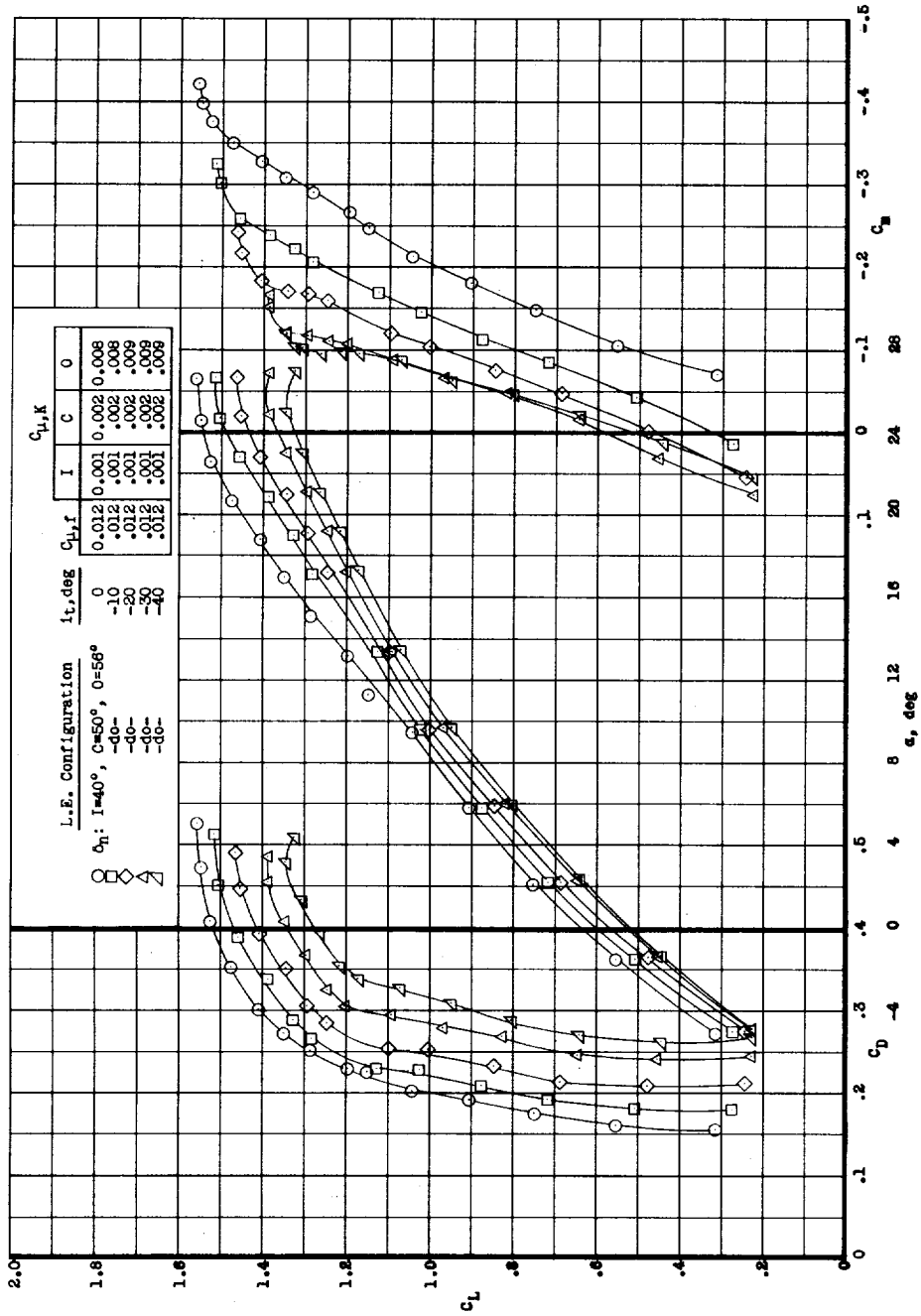

(d) $\beta = -15.18^{\circ}$.

Figure 10.- Concluded.

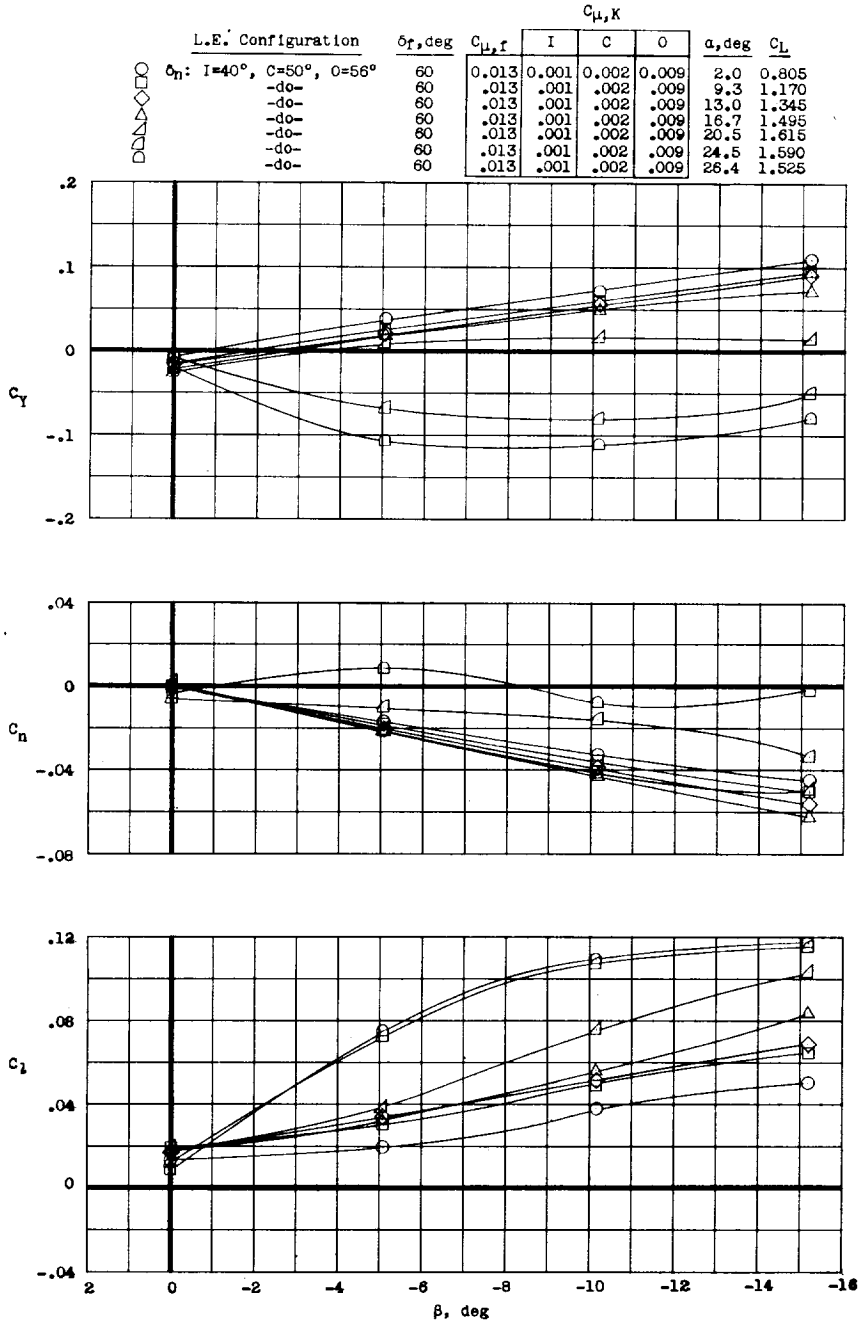

(a) Knee and flap blowing.

Figure 11.- Variation of the static lateral and directional characteristics with angle of sideslip. $\delta_a = 0°$; $i_t = 0°$.

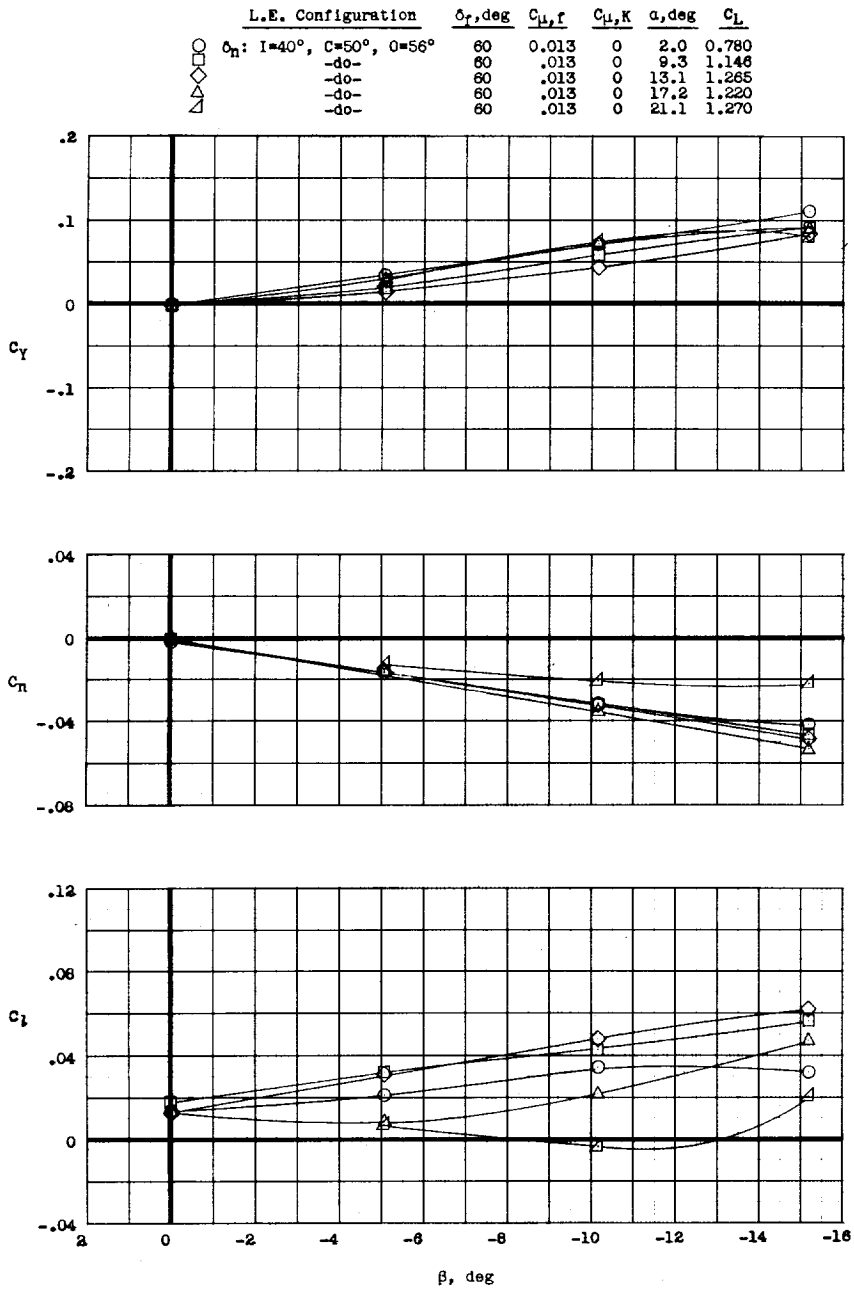

(b) Flap blowing only.

Figure 11.- Continued.

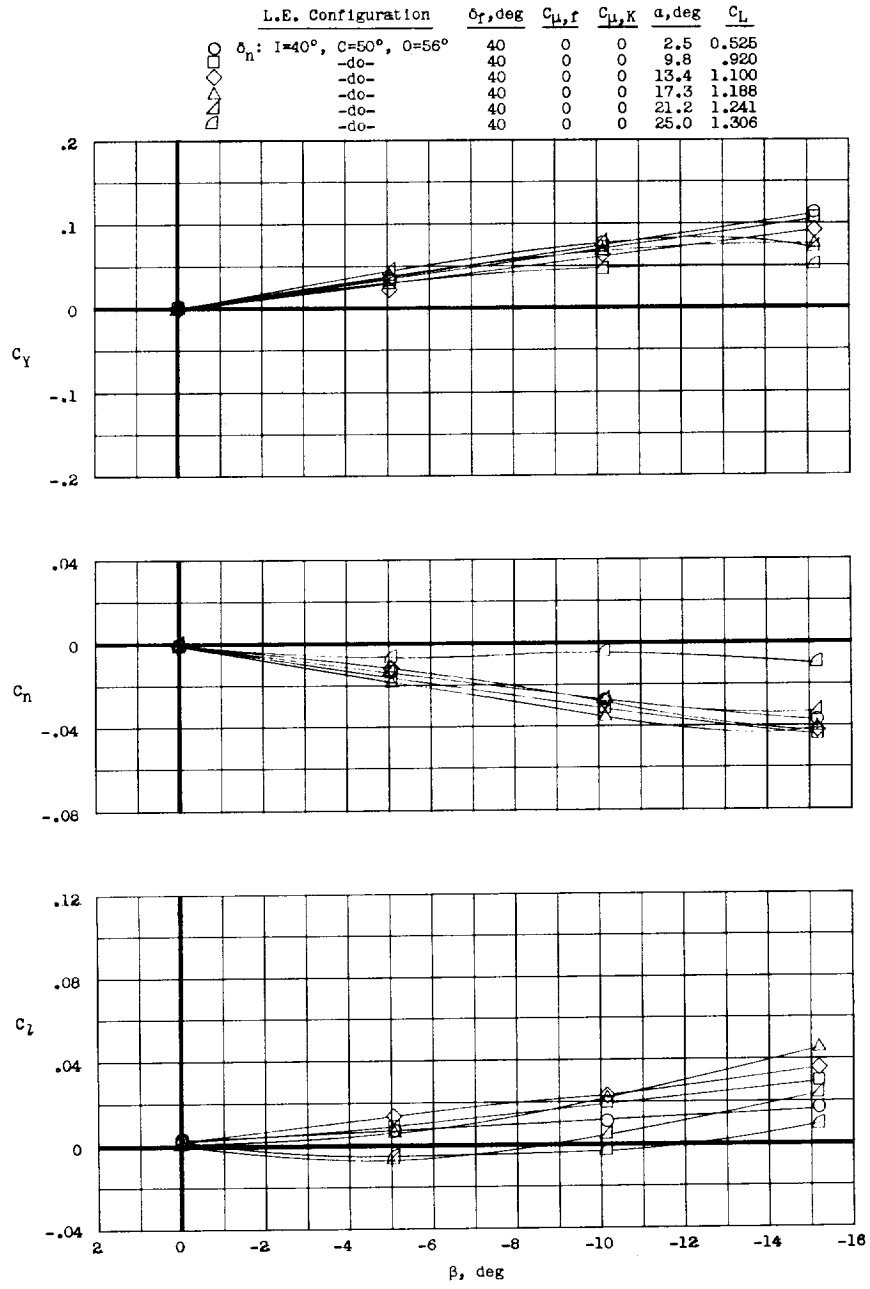

(c) No boundary-layer control.

Figure 11.- Concluded.

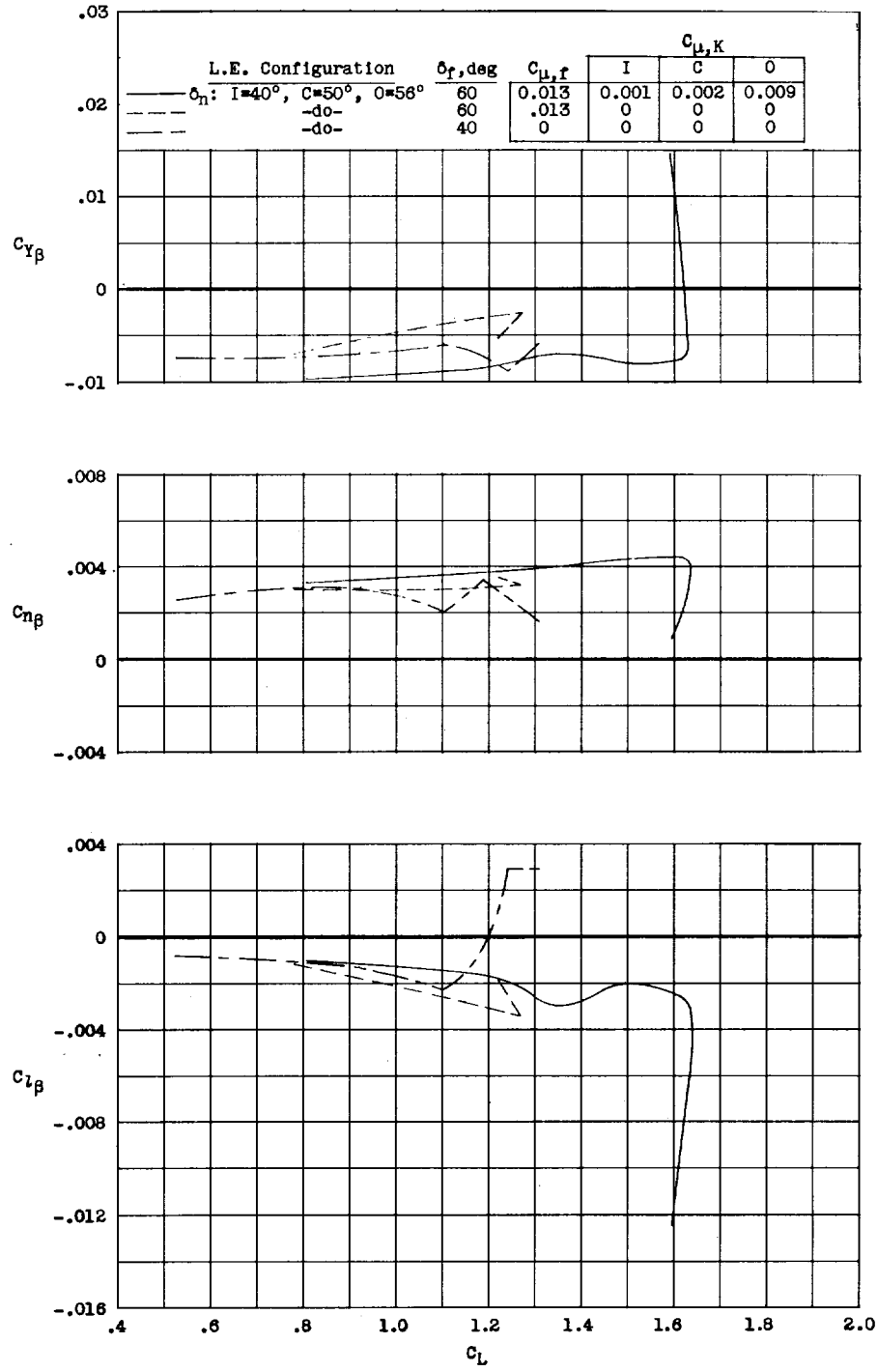

Figure 12.- Static lateral and directional stability characteristics with and without boundary-layer control. $\delta_a = 0^o$; $i_t = 0^o$.

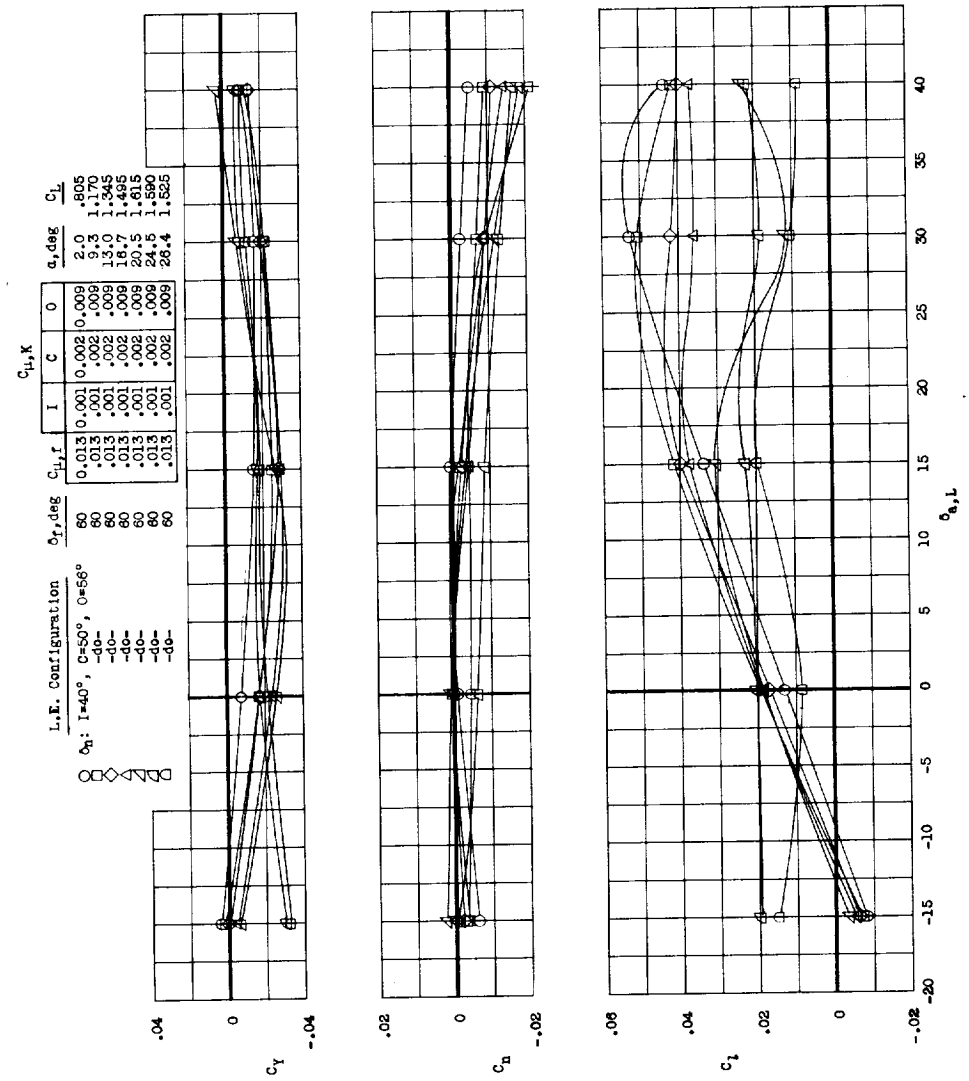

(a) Knee and flap blowing.

Figure 13.- Variation of the static lateral and directional characteristics with aileron deflection with and without boundary-layer control. $\beta = 0^\circ$; $i_t = 0^\circ$.

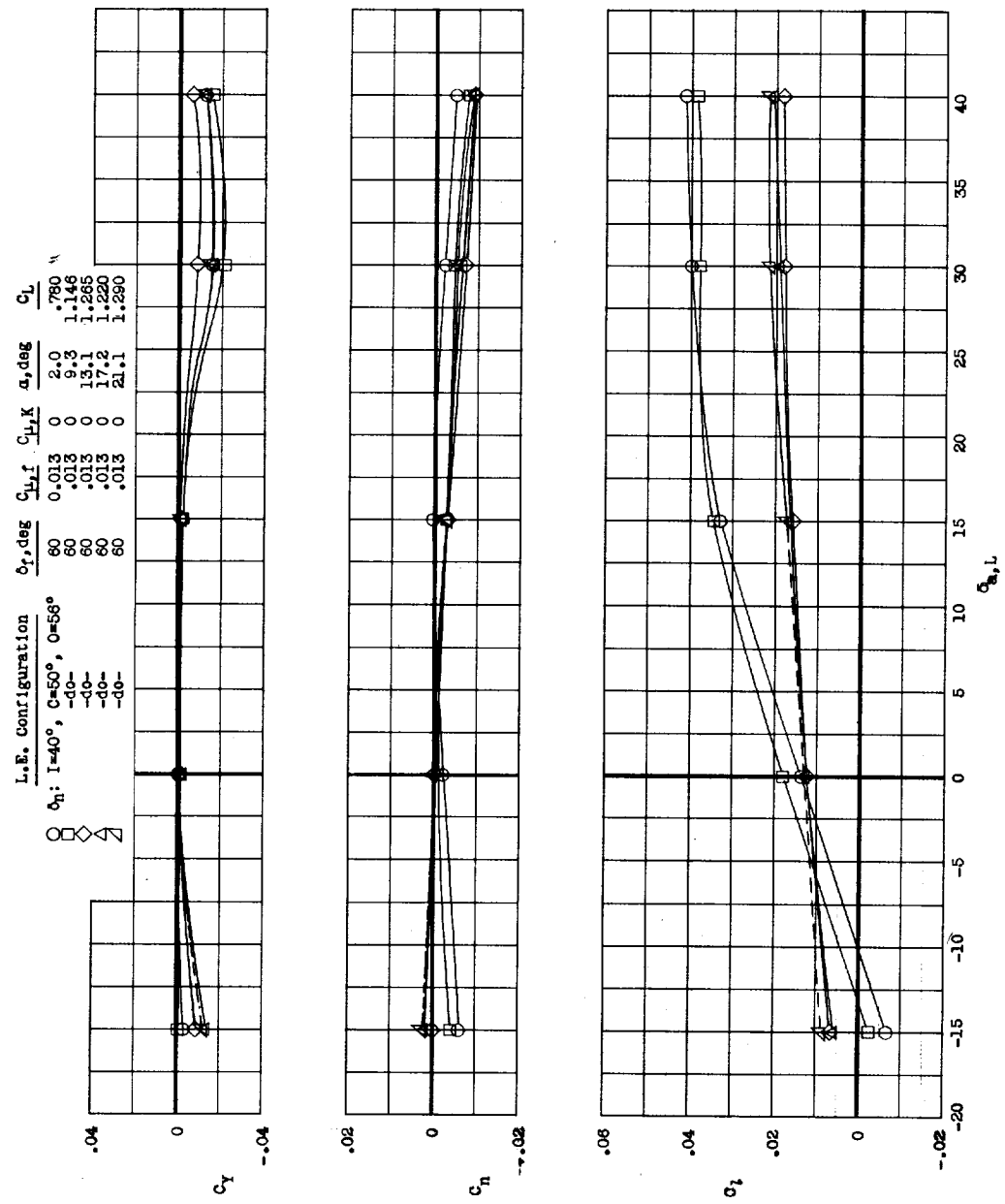

(b) Flap blowing only.

Figure 13.- Continued.

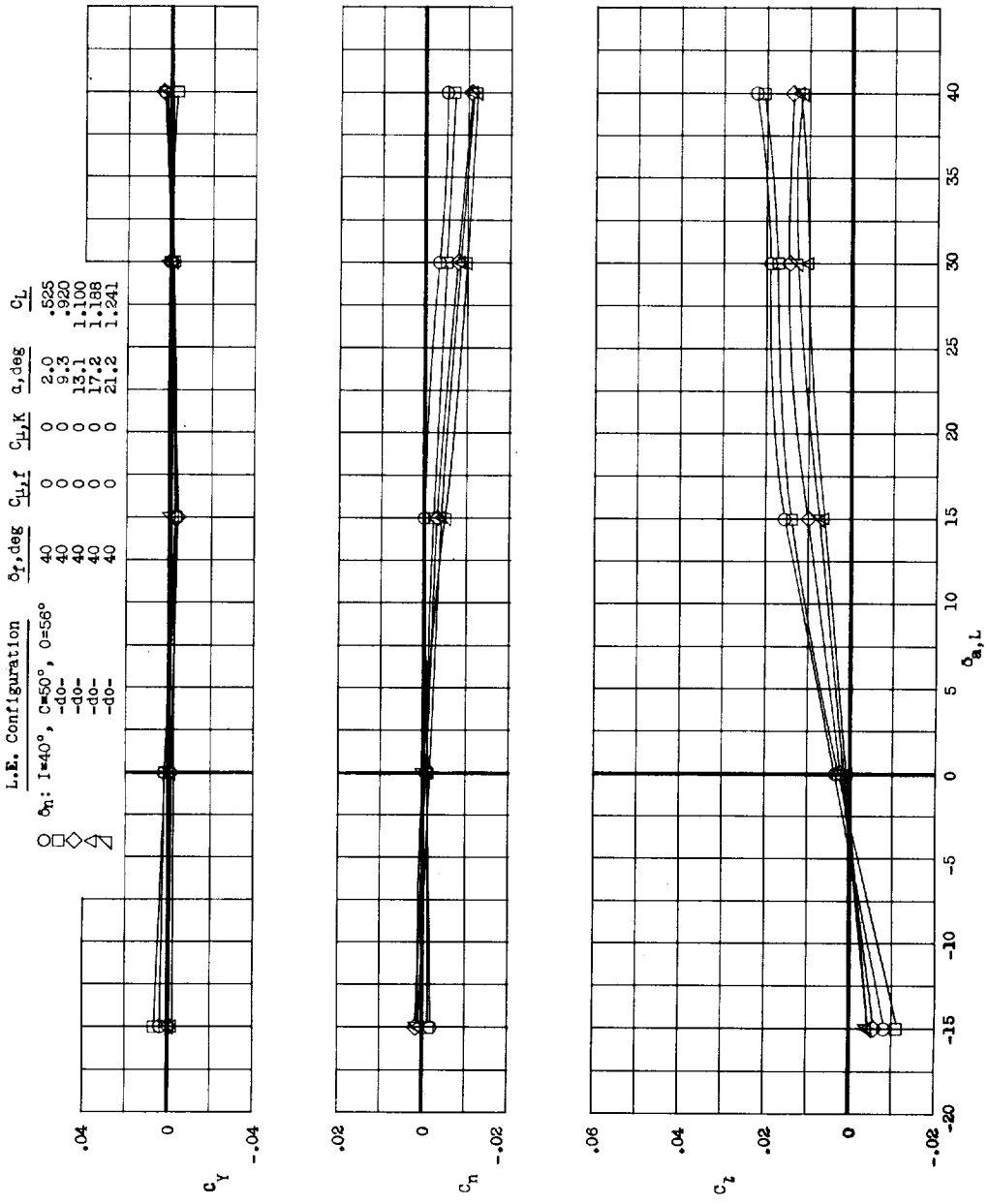

(c) No boundary-layer control.

Figure 13.- Concluded.

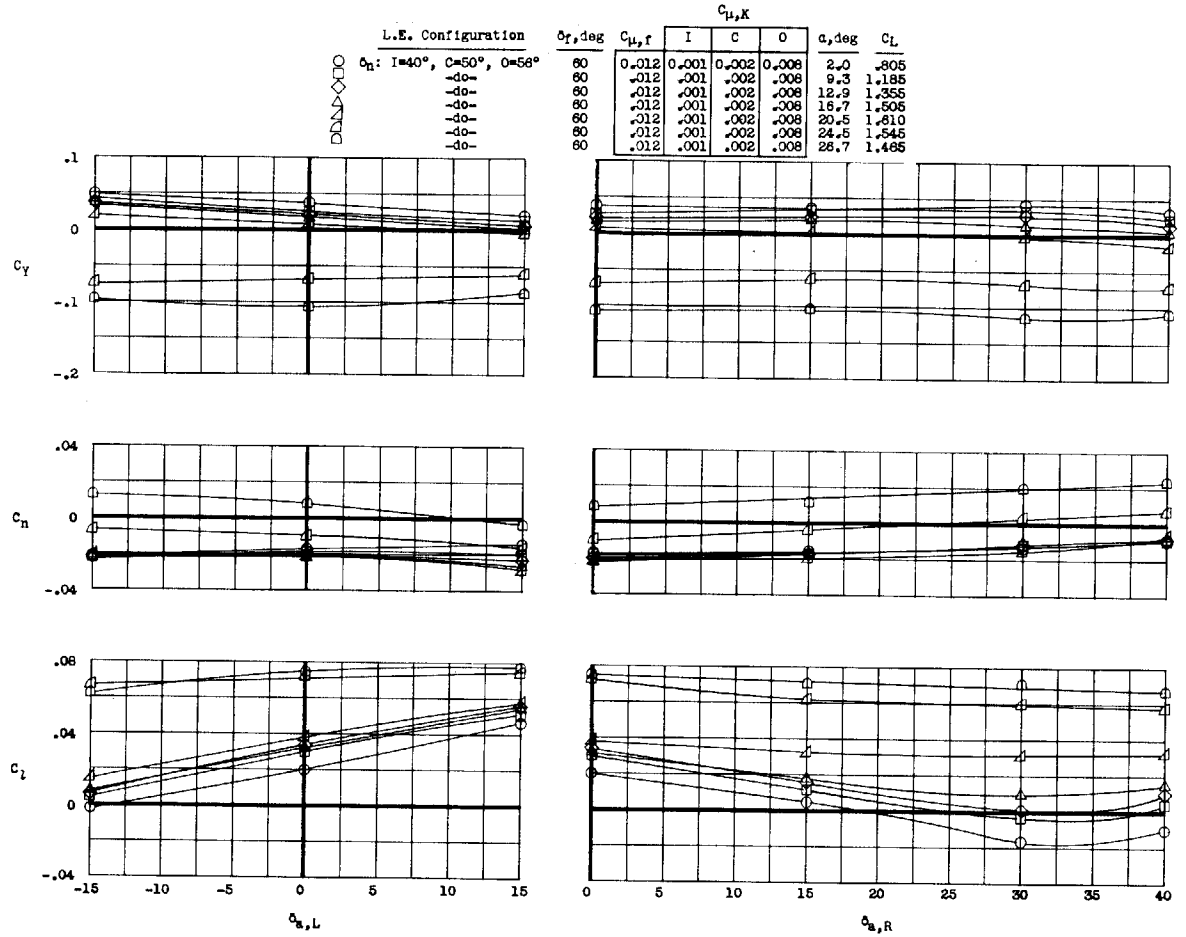

(a) Knee and flap blowing.

Figure 14.- Variation of the static lateral and directional characteristics with aileron deflection with and without boundary-layer control. $\beta = -5.06^{\circ}$; $i_t = 0^{\circ}$.

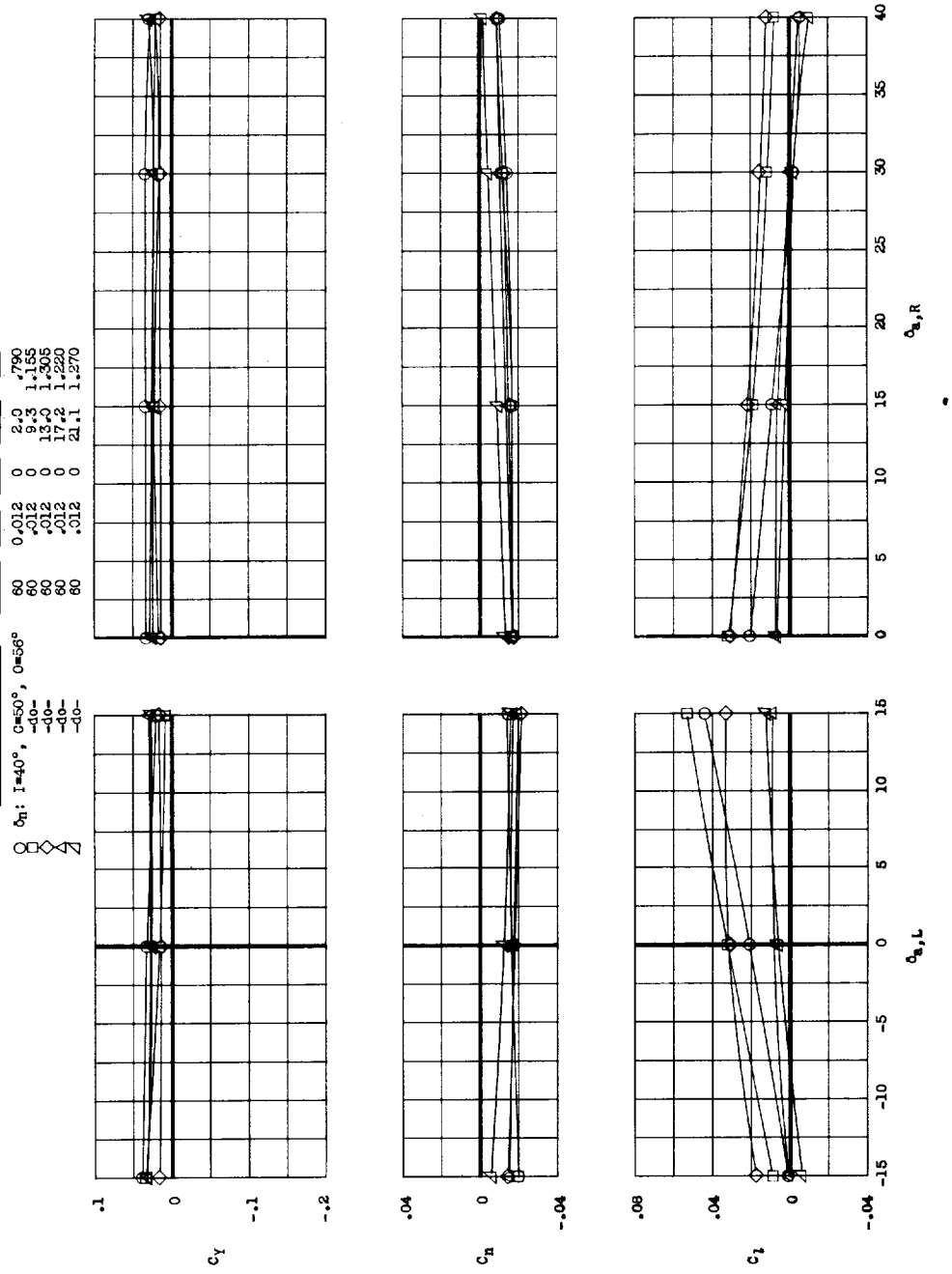

(b) Flap blowing only.

Figure 14.- Continued.

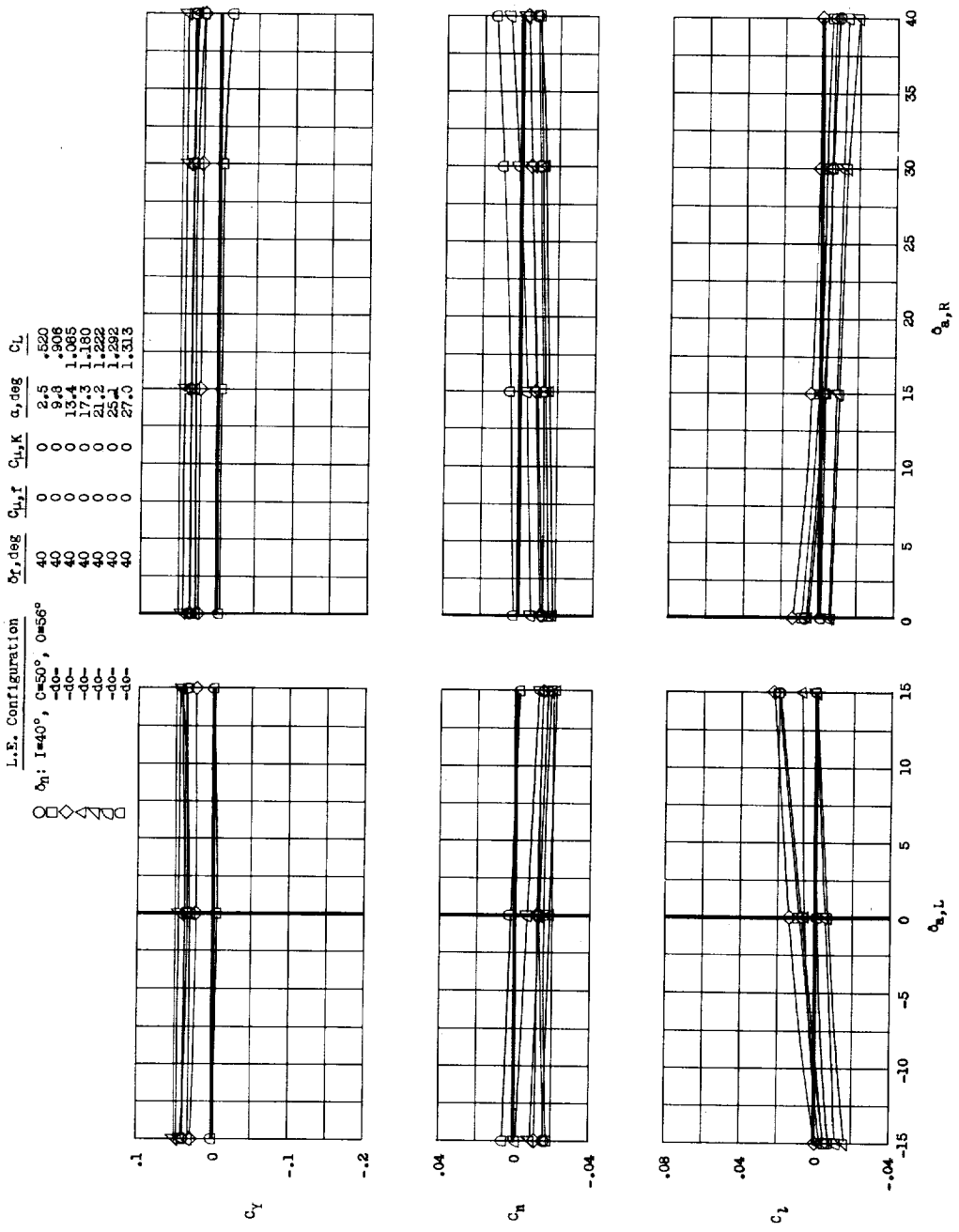

(c) No boundary-layer control.

Figure 14.- Concluded.

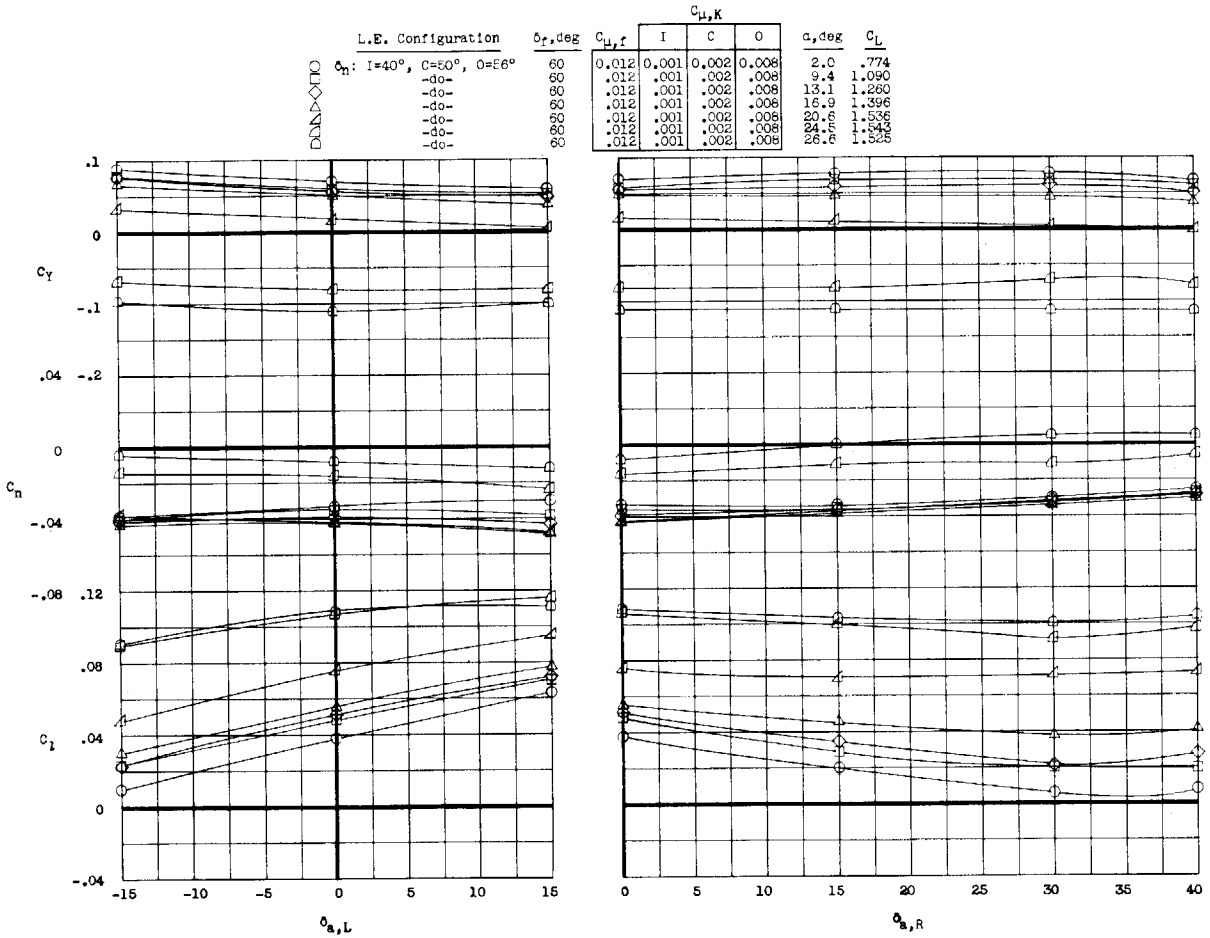

δ_f,deg	$C_{\mu,f}$	$C_{\mu,K}$ I	$C_{\mu,K}$ C	$C_{\mu,K}$ O	α,deg	C_L
60	0.012	0.001	0.002	0.008	2.0	.774
60	.012	.001	.002	.008	9.4	1.090
60	.012	.001	.002	.008	13.1	1.260
60	.012	.001	.002	.008	16.9	1.396
60	.012	.001	.002	.008	20.6	1.536
60	.012	.001	.002	.008	24.5	1.543
60	.012	.001	.002	.008	26.6	1.525

(a) Knee and flap blowing.

Figure 15.- Variation of the static lateral and directional characteristics with aileron deflection with and without boundary-layer control. $\beta = -10.15^{\circ}$; $i_t = 0^{\circ}$.

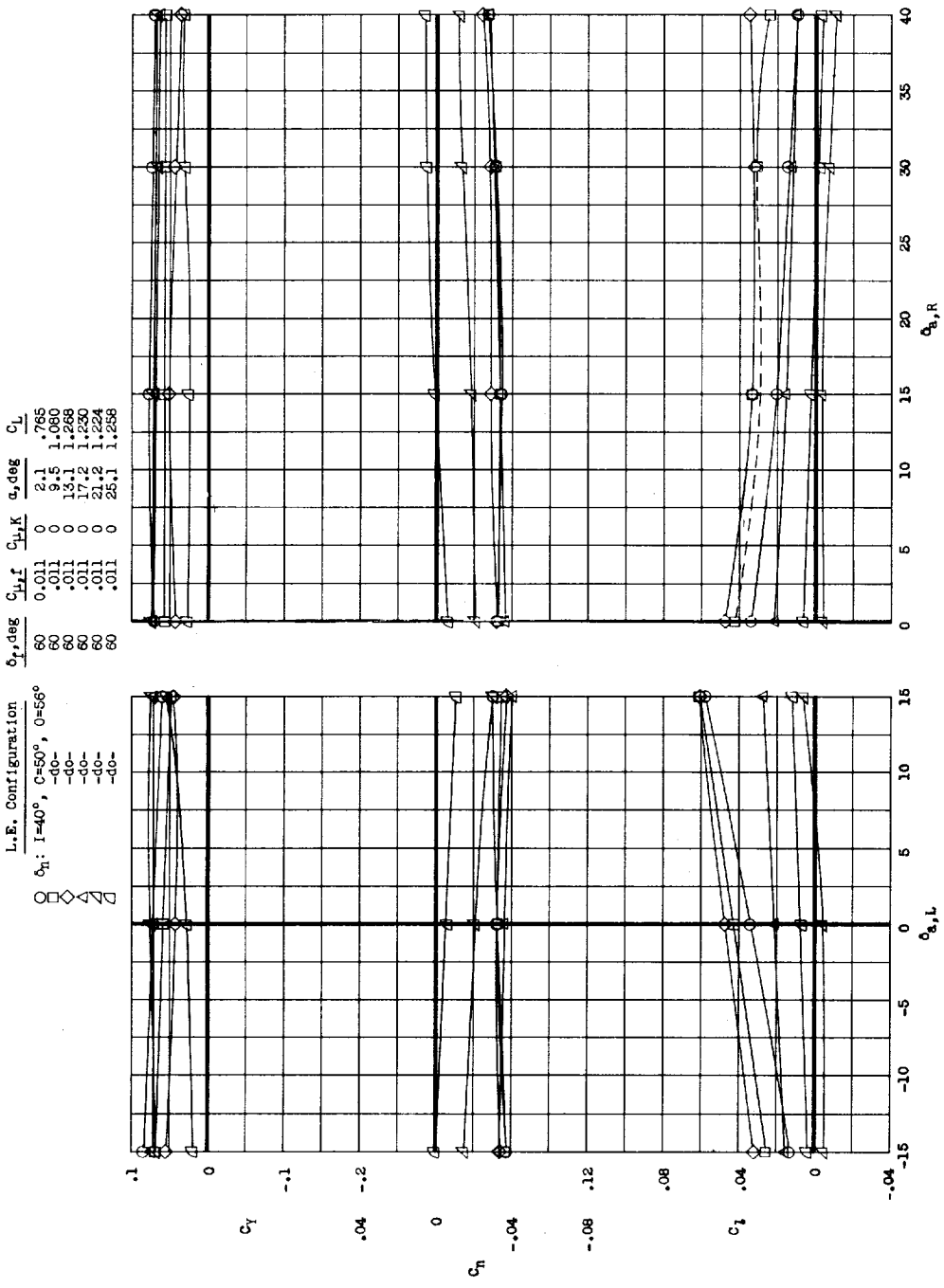

(b) Flap blowing only.

Figure 15.- Continued.

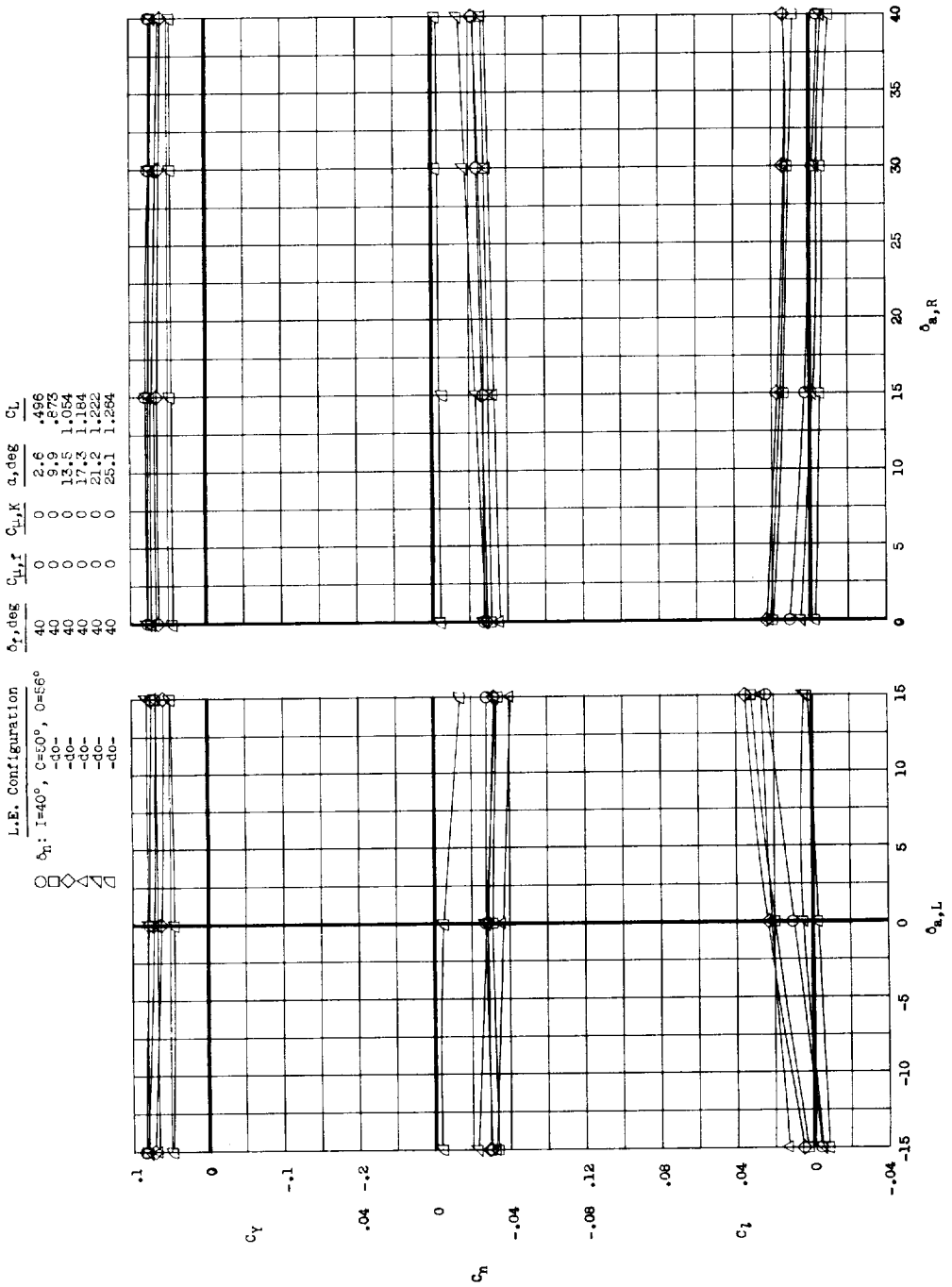

(c) No boundary-layer control.

Figure 15.- Concluded.

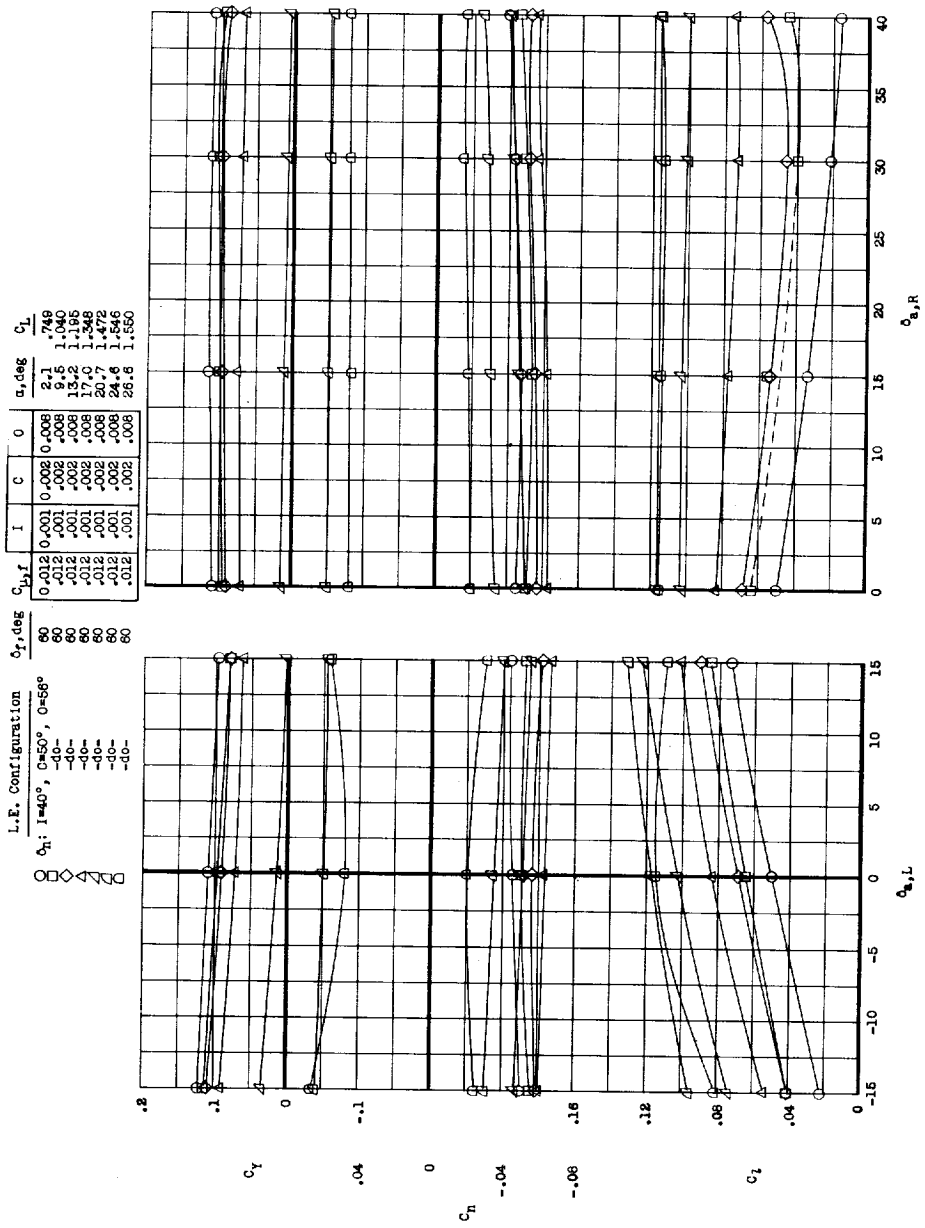

(a) Knee and flap blowing.

Figure 16.- Variation of the static lateral and directional characteristics with aileron deflection with and without boundary-layer control. $\beta = -15.18°$.

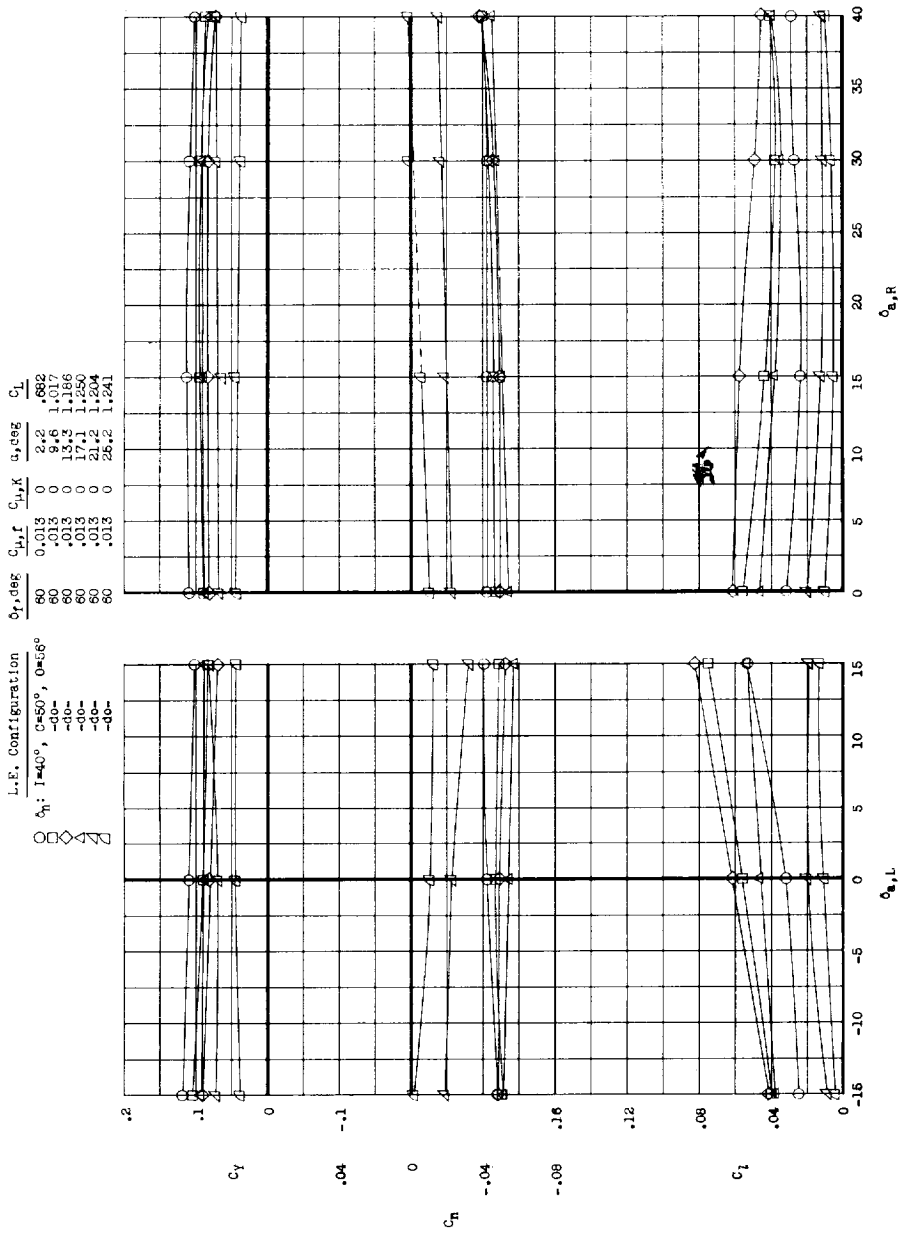

(b) Flap blowing only.

Figure 16.- Continued.

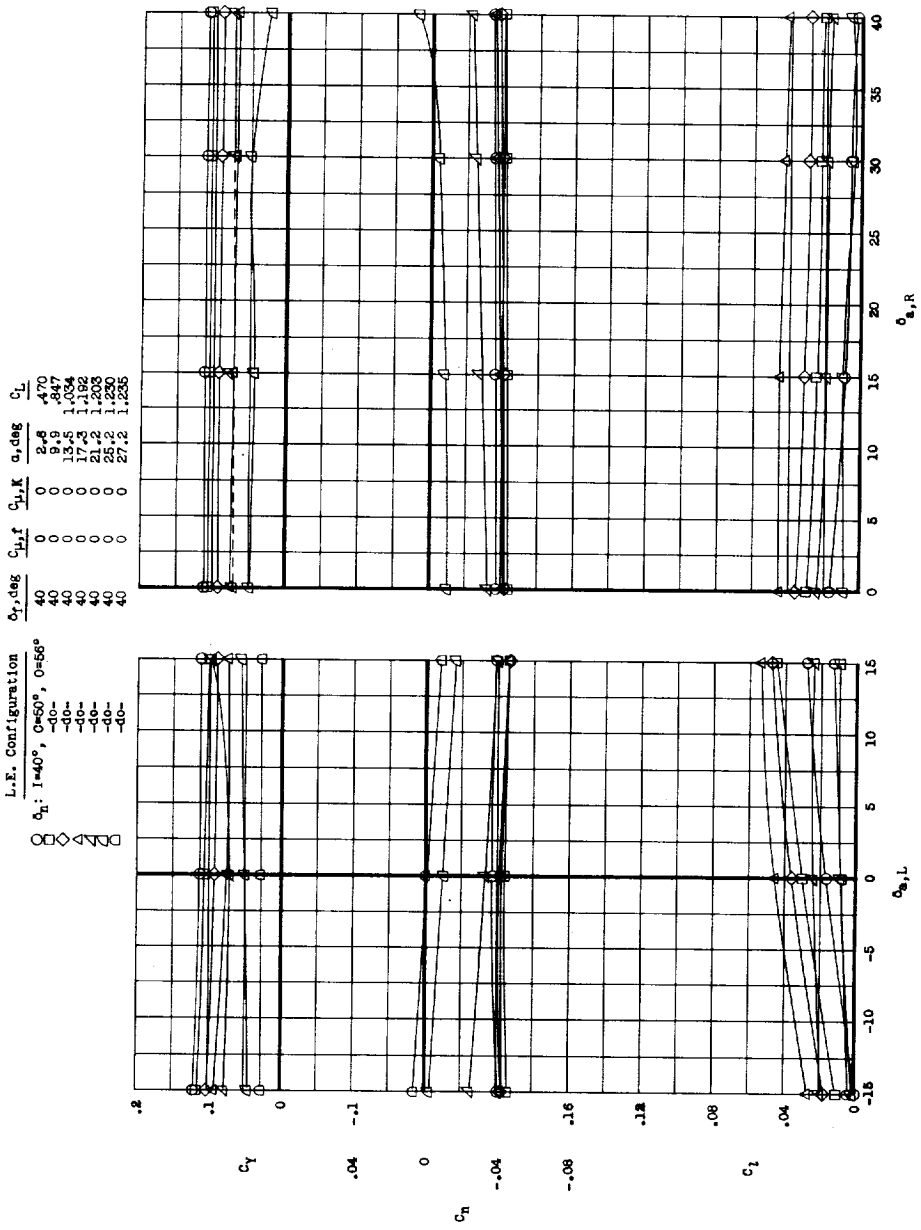

(c) No boundary-layer control.

Figure 16.- Concluded.

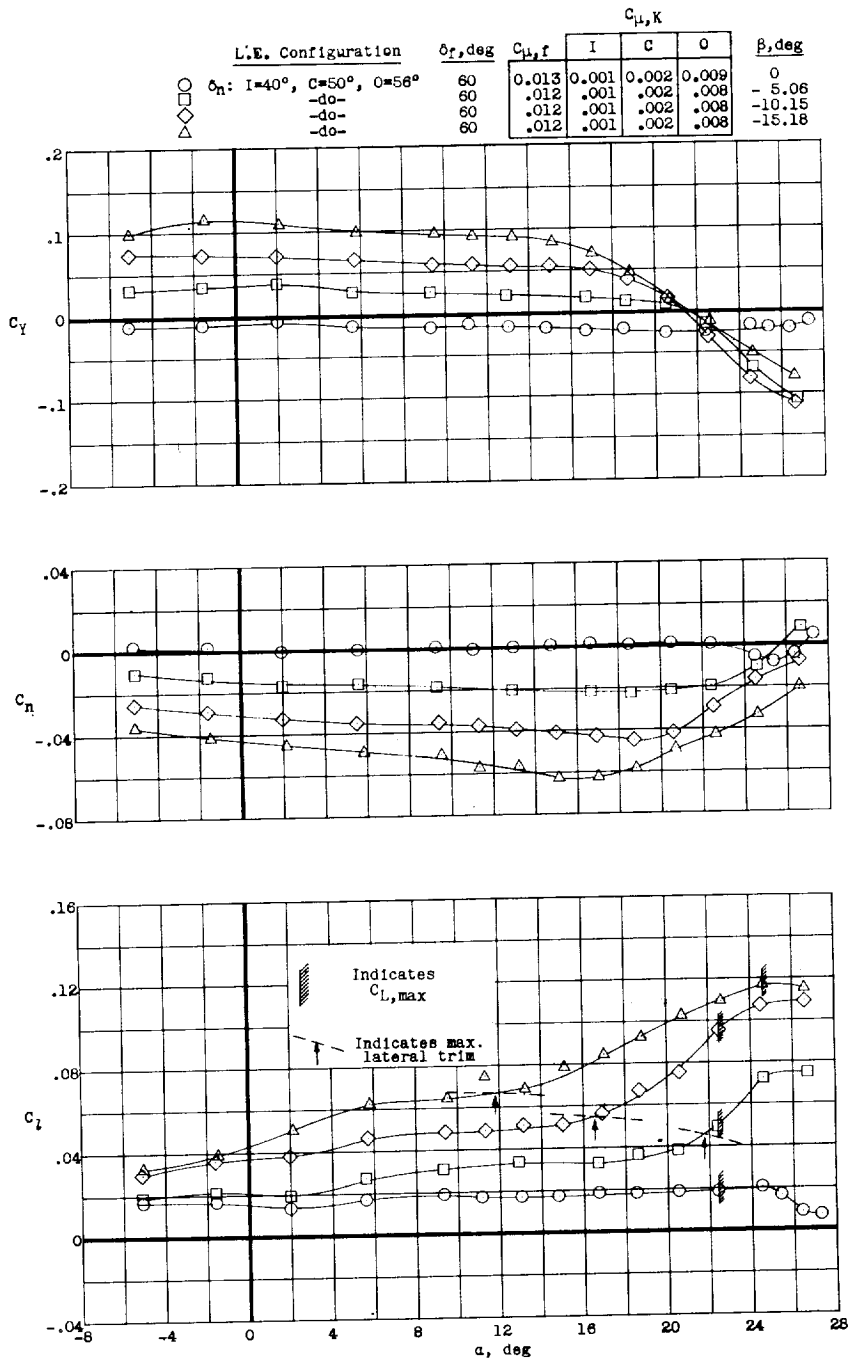

Figure 17.- Variation of the static lateral and directional characteristics with angle of attack for several sideslip angles. $\delta_a = 0^\circ$; $i_t = 0^\circ$.

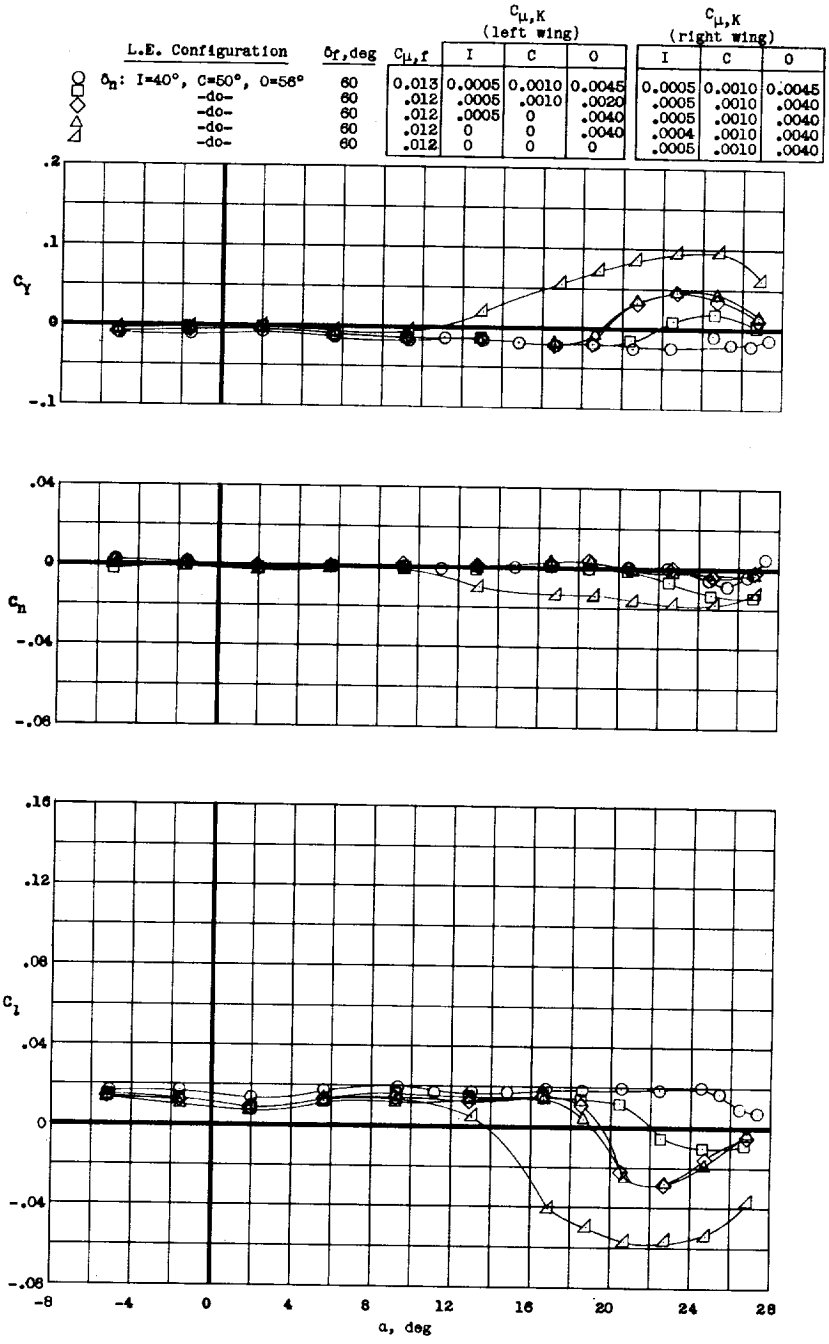

(a) $\beta = 0^{\circ}$.

Figure 18.- Variation of the static lateral characteristics with various rates of knee blowing over the left-hand wing. Knee and flap blowing; $\delta_a = 0^{\circ}$; $i_t = 0^{\circ}$.

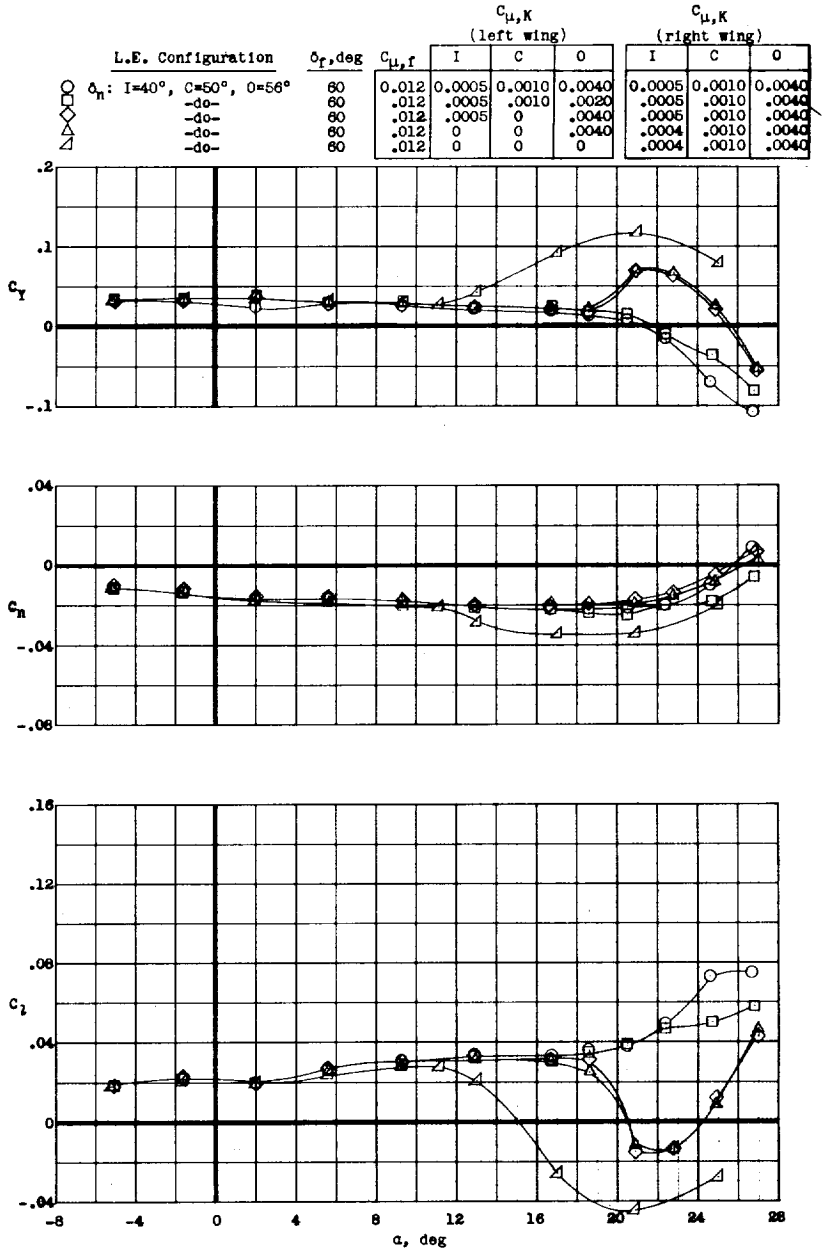

(b) $\beta = -5.06^{\circ}$.

Figure 18.- Continued.

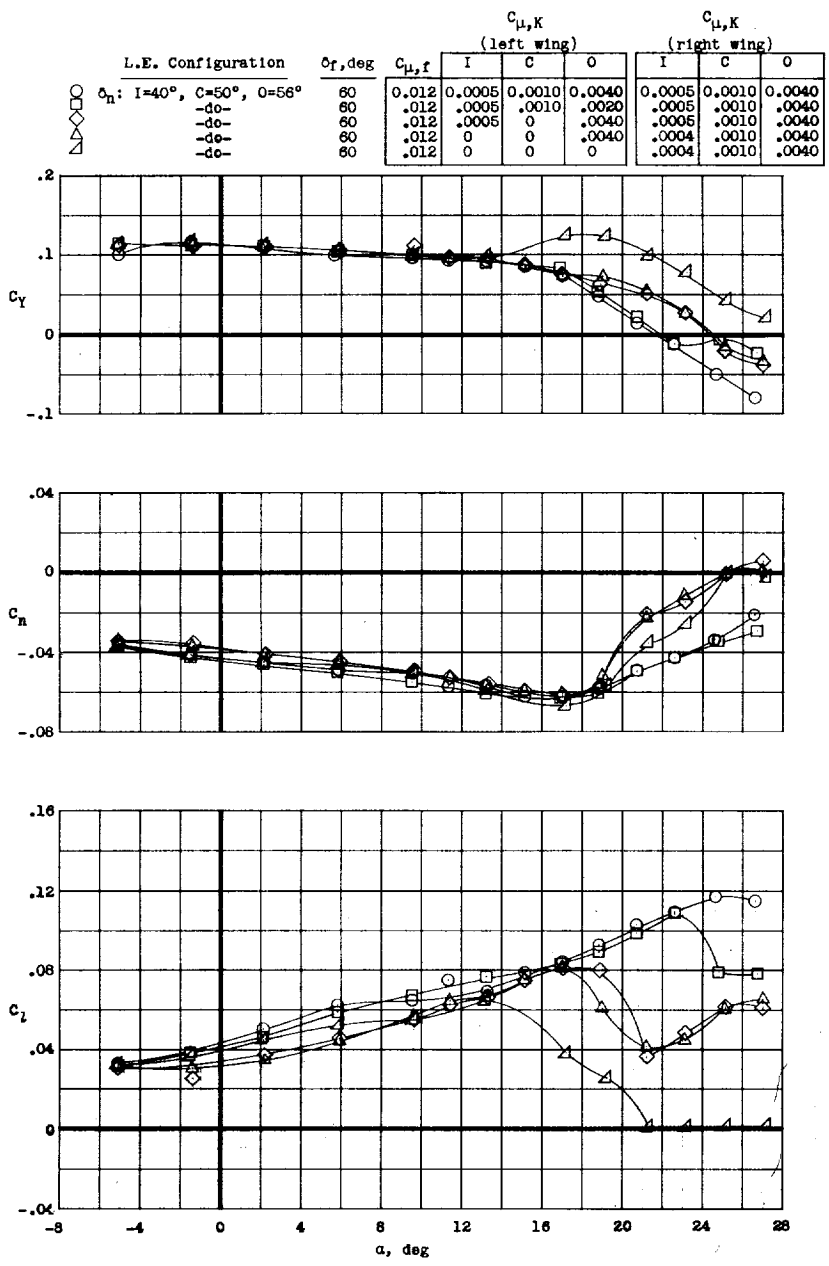

(c) $\beta = -15.18^\circ$.

Figure 18.- Concluded.

NASA - Langley Field, Va.

NASA MEMO 10-11-58L
National Aeronautics and Space Administration.
AERODYNAMIC CHARACTERISTICS IN SIDESLIP OF A LARGE-SCALE 49° SWEPTBACK WING-BODY-TAIL CONFIGURATION WITH BLOWING APPLIED OVER THE FLAPS AND WING LEADING EDGE.
H. Clyde McLemore. October 1958. 46p. diagrs., photo. (NASA MEMO 10-11-58L)
(Title, Unclassified)

Tests were conducted in the Langley full-scale tunnel to determine the lateral and longitudinal stability and control characteristics for sideslip angles of 0°, -5.06°, -10.15°, and -15.18°. An optimum blowing configuration was established. All tests were conducted for the complete angle-of-attack range including the stall for a Reynolds number of 5.2 x 10^6, corresponding to a Mach number of 0.08.

Copies obtainable from NASA, Washington

1. High-Lift Devices - Complete Wings (1.2.2.3)
2. Controls - Complete Wings (1.2.2.4)
3. Boundary-Layer Control - Complete Wings (1.2.2.8.2)
4. Stability, Longitudinal - Static (1.8.1.1.1)
5. Stability, Lateral - Static (1.8.1.1.2)
6. Stability, Directional - Static (1.8.1.1.3)

I. McLemore, Huel Clyde
II. NASA MEMO 10-11-58L

NASA

NASA MEMO 10-11-58L
National Aeronautics and Space Administration.
AERODYNAMIC CHARACTERISTICS IN SIDESLIP OF A LARGE-SCALE 49° SWEPTBACK WING-BODY-TAIL CONFIGURATION WITH BLOWING APPLIED OVER THE FLAPS AND WING LEADING EDGE.
H. Clyde McLemore. October 1958. 46p. diagrs., photo. (NASA MEMO 10-11-58L)
(Title, Unclassified)

Tests were conducted in the Langley full-scale tunnel to determine the lateral and longitudinal stability and control characteristics for sideslip angles of 0°, -5.06°, -10.15°, and -15.18°. An optimum blowing configuration was established. All tests were conducted for the complete angle-of-attack range including the stall for a Reynolds number of 5.2 x 10^6, corresponding to a Mach number of 0.08.

Copies obtainable from NASA, Washington

1. High-Lift Devices - Complete Wings (1.2.2.3)
2. Controls - Complete Wings (1.2.2.4)
3. Boundary-Layer Control - Complete Wings (1.2.2.8.2)
4. Stability, Longitudinal - Static (1.8.1.1.1)
5. Stability, Lateral - Static (1.8.1.1.2)
6. Stability, Directional - Static (1.8.1.1.3)

I. McLemore, Huel Clyde
II. NASA MEMO 10-11-58L

NASA

NASA MEMO 10-11-58L
National Aeronautics and Space Administration.
AERODYNAMIC CHARACTERISTICS IN SIDESLIP OF A LARGE-SCALE 49° SWEPTBACK WING-BODY-TAIL CONFIGURATION WITH BLOWING APPLIED OVER THE FLAPS AND WING LEADING EDGE.
H. Clyde McLemore. October 1958. 46p. diagrs., photo. (NASA MEMO 10-11-58L)
(Title, Unclassified)

Tests were conducted in the Langley full-scale tunnel to determine the lateral and longitudinal stability and control characteristics for sideslip angles of 0°, -5.06°, -10.15°, and -15.18°. An optimum blowing configuration was established. All tests were conducted for the complete angle-of-attack range including the stall for a Reynolds number of 5.2 x 10^6, corresponding to a Mach number of 0.08.

Copies obtainable from NASA, Washington

1. High-Lift Devices - Complete Wings (1.2.2.3)
2. Controls - Complete Wings (1.2.2.4)
3. Boundary-Layer Control - Complete Wings (1.2.2.8.2)
4. Stability, Longitudinal - Static (1.8.1.1.1)
5. Stability, Lateral - Static (1.8.1.1.2)
6. Stability, Directional - Static (1.8.1.1.3)

I. McLemore, Huel Clyde
II. NASA MEMO 10-11-58L

NASA

NASA MEMO 10-11-58L
National Aeronautics and Space Administration.
AERODYNAMIC CHARACTERISTICS IN SIDESLIP OF A LARGE-SCALE 49° SWEPTBACK WING-BODY-TAIL CONFIGURATION WITH BLOWING APPLIED OVER THE FLAPS AND WING LEADING EDGE.
H. Clyde McLemore. October 1958. 46p. diagrs., photo. (NASA MEMO 10-11-58L)
(Title, Unclassified)

Tests were conducted in the Langley full-scale tunnel to determine the lateral and longitudinal stability and control characteristics for sideslip angles of 0°, -5.06°, -10.15°, and -15.18°. An optimum blowing configuration was established. All tests were conducted for the complete angle-of-attack range including the stall for a Reynolds number of 5.2 x 10^6, corresponding to a Mach number of 0.08.

Copies obtainable from NASA, Washington

1. High-Lift Devices - Complete Wings (1.2.2.3)
2. Controls - Complete Wings (1.2.2.4)
3. Boundary-Layer Control - Complete Wings (1.2.2.8.2)
4. Stability, Longitudinal - Static (1.8.1.1.1)
5. Stability, Lateral - Static (1.8.1.1.2)
6. Stability, Directional - Static (1.8.1.1.3)

I. McLemore, Huel Clyde
II. NASA MEMO 10-11-58L

NASA